



80 AL
6 Storey's Gate
Westminster
London
SW1P 3AU

Telephone 01-222 3891
Facsimile 01-222 3700

THE RESEARCH AND INFORMATION GROUP FOR THE UNDERWATER AND OFFSHORE ENGINEERING INDUSTRIES

CONFIDENTIAL TO URP/72 PARTICIPANTS

UEG Joint Industry Project on
Underwater Inspection

FINAL REPORT ON

Probability Based Fatigue Inspection Planning

by

Dr. H. Madsen
Veritas Research

August, 1988

LIST OF CONTENTS

0. Summary	2
1. General overview/introduction to the probabilistic approach	4
2. Review of current data on reliability of inspection methods	7
3. Presentation of case study	10
4. Appraisal of the limitations of the study	34
5. References	36
APPENDIX	

SUMMARY

This report presents results from one of several studies on various inspection related topics which form the UEG Project on Underwater Inspection (Project URP72).

A probabilistic fatigue analysis of a hot spot in a tubular joint has been performed to demonstrate the applicability of probabilistic methods to fatigue analysis and inspection planning.

Both a probabilistic S-N fatigue analysis and a probabilistic fracture mechanics fatigue analysis are performed. The two approaches give very similar results and are in principle equivalent provided corresponding input data are applied. An improved quality is desirable in the data background for some input parameters to the fracture mechanics analysis.

It is demonstrated that the probabilistic fracture mechanics analysis is easily combined with results from inspection. The inspection results allow updated failure probabilities to be computed. Uncertainty in inspection methods is required in the form generally available, i.e., in probability of detection curves and in measurement uncertainty in crack sizing.

Based on the probabilistic fatigue analysis the nominal reliability level against fatigue failure in present deterministic design standards is determined. For details designed to the highest standard, i.e., with no inspection or repair possible, the reliability level is close to levels found in studies on static failure.

The most important source of uncertainty in the probabilistic S-N fatigue analysis is the uncertainty in the location of the S-N curve. In the fracture mechanics analysis the uncertainty in the crack growth material parameters is most important.

A review of current data on reliability of inspection methods is disappointing. Data are scarce, data refer to capability rather than performance, and data are almost exclusively on detection probabilities, with only few data on sizing uncertainty.

A study of the effect of different inspection procedures has been performed. The study indicates that a large potential for economic savings in inspection for fatigue cracks in offshore steel structures can be documented through use of probabilistic methods.

In an appraisal of the analysis the most important shortcomings are stated as:

- There is a lack of good data for material crack growth parameters.
- The quality of current data on reliability of performance of inspection methods is poor.
- Target reliability levels must be defined by users or authorities.

- To fully achieve the potential in economic savings by use of probabilistic methods for inspection planning, procedures must be available to evaluate the importance of each element on the system reliability.

1. GENERAL OVERVIEW/INTRODUCTION TO THE PROBABILISTIC APPROACH

The objectives of this study are:

1. To demonstrate the applicability of probabilistic methods to inspection planning.
2. To ascertain the importance/sensitivity of the principal input parameters for the probabilistic analysis.
3. To investigate the effect of different inspection regimes on the reliability of a structural component.
4. To identify shortcomings in currently available probabilistic methods for application to real structures.

The study is aimed at an existing platform and does not cover design where an initial inspection plan is decided upon together with materials, dimensions, etc.

The use of probabilistic methods in structural design is rapidly growing. There is now a general agreement on the philosophy behind use of probabilistic methods in decision making, modeling tools for uncertainty modeling are accepted and unified, and numerical techniques have been developed to compute failure probabilities and sensitivity factors efficiently. Such computer programs are now commercially available and easy to use for many engineers. A general overview and introduction to the probabilistic approach to structural design is presented here, while a more detailed account for the available methods is presented in Madsen et al [1].

A probabilistic approach is applied for different aspects of design. Probabilistic methods are used for calibration of safety factors in structural codes and technical standards. The first such calibration was for the 1974 Canadian Standards Association Code, and since then almost all major codes for land based and offshore structures have been through a formal calibration process. In recent years probabilistic methods have also been used directly as a design tool. This has taken place for failure modes with little previous experience, very important structures either very costly or with very large failure consequences, and for structures which are produced in large numbers. Very recently, the probabilistic methods have been further developed to account for new information becoming available after the design process. Such information is from fabrication, e.g. compliance control of materials, and from service experience. Inspection and monitoring as well as proof loading provide important additional information. With the additional information much of the uncertainty present at the design stage is removed and improved decisions on e.g. repair, strengthening, inspection plan and change in use can be made. This is generally not possible to nearly the same extent only based on the deterministic methods. The application of updating takes place for e.g. bridges, where loads increase due to heavier vehicles being allowed, and this report presents the application for inspection of offshore steel structures.

The use of a probabilistic approach for reliability updating based on inspection results is based on the same concepts and notions as applied in the use for design. The fundamental notion in both deterministic and probability based structural design is the limit state function which gives a discretized assessment of the state of a structure or structural element as being either failed or safe. The limit state function is obtained from a traditional deterministic analysis, but uncertain input

parameters are identified and quantified. The uncertainty in the deterministic load and response models themselves is also attempted quantified. Sources of uncertainty can be inherent physical uncertainty, statistical uncertainty due to estimation of statistical parameters from a small data base, and model uncertainty. All uncertainties are, however, treated in the same way in the analysis independent of their origin.

Sometimes a distinction between randomness and uncertainty is introduced, where the randomness is inherent while the uncertainty in principle can be removed. It must, however, be realized that the classification is not fundamental but related to a level of modeling. Also, the classification depends on the phase of a project. Whereas, e.g., the steel quality of a member is random at the design stage due to a lack of knowledge in the choice of supplier and randomness within the production of the supplier, the steel quality is uncertain in the as-built structure where it can be determined through measurement.

The probability of malfunction or failure is computed by specially devised numerical techniques known as first- and second-order reliability methods. Besides computing probabilities of failure, these methods give a number of important sensitivity factors in addition. The total uncertainty is divided on the different sources indicating where to most effectively allocate resources to reduce uncertainty. Parametric sensitivity factors give the sensitivity of the reliability to changes in design parameters and statistical input parameters. When an initial lay-out is available, but the reliability is not at the target level, these factors give the necessary change in an input parameter to achieve the desired level. No reanalysis is thus necessary when a small change in input is made but the modified reliability is computed directly from the initial analysis.

Because the uncertainties in the input parameters are partly objective and partly subjective the computed failure probability can not be taken as an expected frequency of failure. Rather, the failure probability is a measure of the designers belief in the reliability. As such the failure probabilities may change as more information becomes available. The computed failure probability is therefore not a physical property of the structure.

The structural reliability analysis does not attempt to account for failures due to gross error. Such errors probably cause 90% of all failures. To reduce the frequency of gross error failures by increasing load and resistance factors is, however, not economic, but other means must be used. Such means may well be much more costly than increasing dimensions by a few percent. The ratio of approximately 10:1 between costs of gross error failure and failure due to exceedance of design criteria is therefore not necessarily far from being optimal.

Structural reliability methods have mainly been applied for individual failure modes of single elements in a structure. In recent years an increased interest in system reliability has arisen. It is now possible to compute failure probabilities for general systems - the difficult and as yet not fully solved part is to model a structure with its failure modes as a system in reliability analysis terms.

This report first gives a review of current data on reliability of inspection methods and numerical values are suggested for the probability of detection function

for under water MPI and close visual inspection. The objectives of the study are then highlighted through an example study of a hot spot in a K-joint. Finally, a section identifies shortcomings in currently available probabilistic methods for application to real structures.

2. REVIEW OF CURRENT DATA ON RELIABILITY OF INSPECTION METHODS

Selected conclusions and recommendations from the study of Gray [2, section 10] are:

7. An overly optimistic view (of inspection reliability) is held by many engineers based on their experience of that which has been detected and naturally not what was missed and is therefore unknown.
8. Quantitative data relevant to the reliability of structural inspection methods is generally lacking but those studies carried out indicate reliabilities significantly below those anticipated.
9. The "state-of-the-art" of fracture mechanics is now developing ahead of that of inspection reliability such that the potentially sensitive defect assessments are severely limited by the reliability of the inspection methods used, e.g. UE (ultra-sonic examination).
10. Most studies have assessed the capability rather than the actual performance that should be expected of an inspection method in normal use.
12. Where NDE reliability trials are carried out on simple geometries, with an unnaturally high occurrence of defects, with high vigilance and without access problems, fatigue, contractual pressures etc., true performance on real inspections may be significantly less than the capability demonstrated. True performance needs to be quantified for structural reliability analysis.
15. Due to the dearth of data on inspection reliability, particularly methods other than UE, it is not possible or sound to conclude figures for the reliability of individual inspection methods but certain trends are evident for all methods.
16. Whilst visual inspection appears to be acceptably reliable for the detection of gross errors and damage, it cannot be relied upon to detect cracks unless these are associated with significant opening or are delineated by corrosion products or leakage.
17. It seems reasonable to assume that MPI (Magnetic particle inspection) is likely to detect, i.e. with more than 80% probability, a crack which is longer than 10 mm. The number 10 mm may be 30 mm under water. However, poor procedures and procedure control would give poorer results and there is inadequate data to confirm this assumption.
18. UE performance has not been adequately quantified to date but capability assessments indicate that even under controlled conditions, i.e., trials, there are substantial differences in the performance of different operators. As an example, in one study it was seen that nearly half the operators showed a 40% probability of accepting 10-12 mm high defects in a 26 mm plate.

Other data indicated that POD (probability of detection) of defects in more complex joints, e.g. nozzles and nodes, may be as low as less than 50%, regardless of defect height. The length of defects relative to the inspected length will effect detection performance. The relationship between height and length in POD has not been studied. Attempts to quantify true performance in real inspections

have not been made. It is concluded that "one-off" ultrasonic examinations under the circumstances of current practice on marine structures are likely to give poor detection and characterization performance.

19. RE (radiographic examination) appears to be reliable at detecting "workmanship" defects e.g. slag, porosity and lack of penetration. RE can, however, not be relied upon to detect planar defects, e.g. cracks and lack of fusion, although if orientation is favourable or lack of fusion is associated with other defects, detection is likely. RE therefore continues to be a powerful quality control tool for detecting "workmanship" defects and providing a record for the subsequent judgement of inspectors.
20. Little or no information exists concerning the reliability of ECE (eddy current examination) and ACPD (AC potential drop) crack measurement applied to marine structures. However, ACPD crack depth measurement appears to be capable of performing, with errors, approximately $\pm 10\%$ of crack depth or ± 2 mm, although more data is required. ECE of welds is reported to be as good as MPI but current practice of sample rechecking with MPI may be creating a situation of abnormally high care and vigilance by NDE operators.

One conclusion is thus that very few data are available, both for establishing probability of detection (pod) curves and on uncertainty in size assessment of detected cracks.

The aim of the case study is to compare the effect of visual inspection and MPI (magnetic particle inspection). Although the confidence in pod curves is not very high the following is judged reasonable for the case study. The probability of detecting a crack with depth greater than a is $P_d(a)$, which is taken as (a in mm)

$$P_d(a) = 1 - e^{-a/1.3}, \quad a > 0$$

$$P_d(a) = 1 - e^{-a/2.6}, \quad a > 0 \quad \text{MPI} \quad (2.1a)$$

$$P_d(a) = 1 - e^{-a/6.5}, \quad a > 0$$

$$P_d(a) = 1 - e^{-a/13}, \quad a > 0 \quad \text{visual} \quad (2.1b)$$

Two POD curves for each of the inspection methods are thus provided as shown in Fig. 2.1. Some of the POD curves show a non-negligible probability of not detecting a failure, which in the example is defined as crack growth through the 22 mm wall thickness.

The POD curves in Eq.(2.1) relate to the probability of detection for a specified crack depth. Most inspection methods rely on the possibility of observing the crack length. There is not a perfect correlation between the crack length and the crack depth. This applies both immediately after fabrication where inspection results show a great deal of scatter in crack depth for a fixed crack length. It also applies for growing cracks, where in particular the ratio between the membrane stress and the bending stress is governing for the development of the aspect ratio, i.e. the ratio between depth a and half length c . A quite different development for an unstiffened joint with a large ratio between bending and membrane stress and a stiffened joint with a smaller ratio is thus present. The crack growth analysis should thus be formulated for a vectorial description (a, c) of the crack size, and the theory and

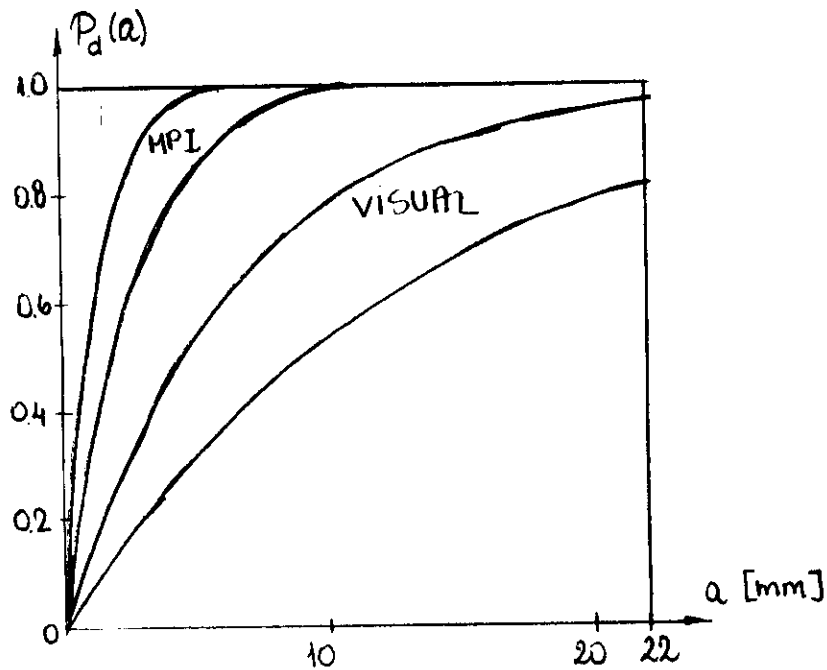


Figure 2.1 POD curves

software applied in the case study has indeed been extended to cover such a description. Most useful information about observed aspect ratios in fatigue tests of tubular joints is reported in DeO [3].

The fatigue crack aspect ratio a/c is often reported near 0.15 for tubular joints. Assuming this ratio the pod curves in Eq.(2.1) give a 90% probability of detecting respectively a 40 mm and 80 mm long crack by MPI and a 90% probability of detecting respectively a 200 mm and 400 mm long crack by visual inspection. Due to the small amount of data on which Eq.(2.1) is based, statistical uncertainty introduced in the constant of the exponential function is relevant. This is, however, not considered here, although it is easily included in the subsequent analysis. The detection of a crack in different inspections is assumed to be statistically independent events.

3. PRESENTATION OF CASE STUDY

Two hot spots in a tubular joint (K-joint) in a jacket structure in shallow water are selected. The following types of analysis are performed and compared:

1. Deterministic fatigue analysis based on Miner-Palmgren fatigue damage accumulation model with S-N curves (DETFAT).
2. Probabilistic fatigue analysis based on Miner-Palmgren fatigue damage accumulation model with S-N curves (PROFAT).
3. Probabilistic fatigue analysis based on Paris fatigue damage accumulation model, i.e. crack growth (PROCRACK).
4. Investigation of the effects of different inspection procedures on the reliability of the joint (PROLONG & PROINSP).

The names in parenthesis are the names of the computer programs (developed at A.S Veritas Research) used in the various analyses. The background theory of the analysis is only briefly discussed in this section. A complete description of the reliability updating is reproduced in the Appendix.

3.1 Deterministic S-N fatigue analysis

This analysis is a standard spectral fatigue analysis and the method and input are briefly described.

A model of the environmental conditions in terms of stationary sea states is applied. In each sea state the sea elevation is modeled as a stationary Gaussian process, characterized by a wave spectrum. Parameters in the wave spectrum describe the main wave direction, significant wave height, mean wave period, wave spectral bandwidth and directional wave energy spreading. A spectrum in terms of direction θ and angular frequency ω is assumed of the form

$$S_{\eta}(\omega, \theta) = W_{\eta}(\omega) \cdot G(\theta) \quad (3.1)$$

$W_{\eta}(\omega)$ is selected as the Pierson-Moskowitz spectrum and $G(\theta)$ is a squared cosine function.

8 main wave directions are used and the fractions of time with each direction are shown in Table 3.1. The fractions of time with each combination of significant wave height H_S and mean wave period T_Z are available from the $H_S - T_Z$ diagram, see Table 3.2. Totally, 41 seastates are included in the analyses. The same diagram is used for all main wave directions.

The wave kinematics are calculated by linear wave theory (Airy) and loads are computed by Morison's equation. The drag loading is linearized and a linear structural analysis (FEM) is performed. A beam model is used with no joint flexibility. Unit height waves of different angular frequency and different direction are applied. As a result, complex transfer functions $H_{\eta F_i}(\omega)$ for section forces and moments $F_i(t)$ in each beam end are determined.

Wave approach from	Probability of occurrence
N	0.0956
NE	0.0689
E	0.0857
SE	0.1179
S	0.1118
SW	0.1698
W	0.1748
NW	0.1755

Table 3.1 The directional distribution of wave occurrences.

H_S [m]	T_Z (zero up-crossing period) [sec]										
	1-2	2-3	3-4	4-5	5-6	6-7	7-8	8-9	9-10	10-11	SUM
0-0.5	0	9	74	19	1	0	0	0	0	0	113
0.5-1.0	0	0	62	163	31	3	0	0	0	0	259
1.0-1.5	0	0	0	112	93	16	3	0	0	0	224
1.5-2.0	0	0	0	13	89	31	7	1	0	0	141
2.0-2.5	0	0	0	0	49	45	6	1	0	0	101
2.5-3.0	0	0	0	12	61	9	2	0	0	0	82
3.0-3.5	0	0	0	0	0	29	11	1	0	0	41
3.5-4.0	0	0	0	0	0	8	11	1	0	0	20
4.0-4.5	0	0	0	0	0	2	8	2	0	0	12
4.5-5.0	0	0	0	0	0	0	5	1	0	0	6
5.0-5.5	0	0	0	0	0	0	2	2	0	0	4
5.5-6.0	0	0	0	0	0	0	2	1	1	0	4
SUM	0	9	136	307	275	195	64	12	1	0	1000

Table 3.2 The sea scatter diagram.

A linear stress analysis of the K-joint with six degrees of freedom fixed is performed, and the hot spot stress for unit loads in each of the remaining 18 degrees of freedom is determined, see Fig. 3.1. The hot spot stress is taken as the component perpendicular to the weld. A linear stress variation over the thickness is assumed as shown in Figure 3.2.

The axial component $\sigma_a(t)$ is expressed in terms of the sectional forces and moments $F_i(t)$ and the influence coefficients $I_{a,i}$, i.e. the axial stress for a unit force or moment in the i th degree of freedom, as

$$\sigma_a(t) = \sum_{i=1}^{18} I_{a,i} F_i(t) \quad (3.2)$$

The bending stress is expressed in a similar manner. As an approximation, only the axial force and bending moments in the brace are included. The axial and bending components $\sigma_a(t)$ and $\sigma_b(t)$ are completely in phase and in the S-N analysis the hot spot stress is taken as

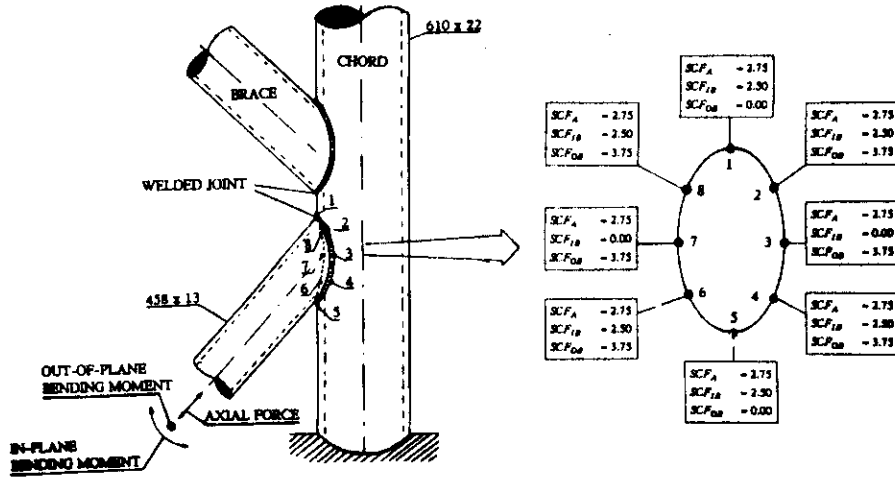


Figure 3.1 Calculation of influence coefficient.

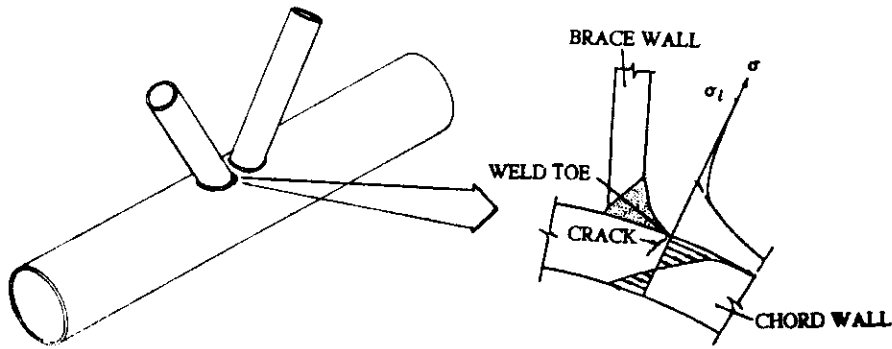


Figure 3.2 Stress variation through thickness.

$$\sigma(t) = \sigma_a(t) + \sigma_b(t) \quad (3.3a)$$

$$I_i = I_{i,a} + I_{i,b} \quad (3.3b)$$

The spectral density of the hot spot stress in a sea state is for a unidirectional sea

$$S_\sigma(\omega) = \sum_{i=1}^{18} \sum_{j=1}^{18} I_i I_j H_{\eta F_i}(\omega) H_{\eta F_j}(\omega)^* S_\eta(\omega) \quad (3.4)$$

where an asterisk denotes a complex conjugate. With wave energy spreading an additional summation over elementary wave directions is performed. The hot spot stress process is assumed Gaussian and narrow banded. Stress ranges then follow a Rayleigh distribution. A better description accounting for the non-Gaussian response due to drag is presented in Skjong and Madsen [4] and is implemented in the applied computer programs.

The fatigue strength is expressed in terms of an S-N curve, giving the number N of stress cycles of constant range S leading to failure. Failure is here defined as crack growth through the wall thickness. The curve from Department of Energy is used both with and without a change in slope at $N = 10^7$ stress cycles, see Figure 3.3 [5].

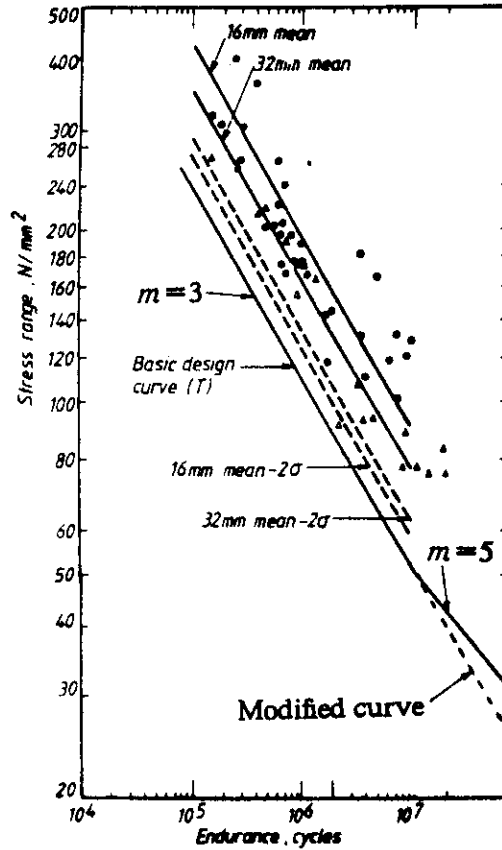


Figure 3.3 Department of Energy T-curve, [5].

The mathematical form of the curve is

$$\log_{10}(N) = 12.16 - 3.0\log_{10}(S) , \quad S \geq 53 \text{ N/mm}^2 \quad (N \leq 10^7) \quad (3.5a)$$

$$\log_{10}(N) = 15.61 - 5.0\log_{10}(S) , \quad S \leq 53 \text{ N/mm}^2 \quad (N \geq 10^7) \quad (3.5b)$$

Without a change in slope the similar form is

$$\log_{10}(N) = 12.16 - 3.0\log_{10}(S) \quad S \geq 0 \text{ N/mm}^2 \quad (3.6)$$

The thickness reduction proposed by Department of Energy is implemented in the applied computer programs. The chord thickness is 22.3 mm and no thickness reduction is performed in the present analysis.

In computing the damage for variable amplitude loading, Miner's rule is applied. The damage increment ΔD_i in a stress cycle of range S_i is according to the rule

$$\Delta D_i = \frac{1}{N(S_i)} \tag{3.7}$$

Damage increments are added independently of the position of a stress cycle in the stress history. Failure is assumed to take place when the damage D exceeds 1.

The total damage is computed as a weighted average of damages from the different sea states. For the S-N curve (3.6) the result is

$$D = \sum_{\theta} \sum_{(H_S, T_Z)} p_i q_j \frac{T}{K} (2\sqrt{2})^3 \nu_{0,ij} \text{Var}[\sigma_{ij}]^{3/2} \Gamma(1 + \frac{3}{2}) \tag{3.8}$$

where T is the length of the considered time period, $p_i q_j$ is the fraction of time with a specific sea state, $\nu_{0,ij}$ and $\text{Var}[\sigma_{ij}]$ are the mean rate of cycles and variance, respectively, in the specific sea state, and $\Gamma()$ denotes the Gamma function. A slightly more complicated expression results from using the T-curve (3.5).

The deterministic life time T corresponding to an accumulated damage of 1 is determined and the results are shown in Table 3.3.

Table 3.3	DETERMINISTIC LIFE TIME IN YEARS	
	T-curve	T-curve modified
Hot spot 1	488	111
Hot spot 2	107	40

Stresses at hot spot 1 are fairly small and the effect on the life time of the change of slope in the S-N curve is large. For hot spot 2 with larger stresses the effect is not as significant.

3.2 Probabilistic S-N fatigue analysis

The probabilistic S-N fatigue analysis uses identically the same models as the deterministic analysis, but the randomness and uncertainty in input parameters is modeled explicitly. It is beyond the scope of this report to give a detailed account of the uncertainty modeling. It suffices to mention that uncertainties are considered in:

- sea scatter diagram
- wave energy spreading function
- wave spectral band width
- load coefficients (transfer functions)
- influence numbers (stress concentration factors)
- location of S-N curves (deterministic slope)
- Miner sum at failure

Some statistical input parameters are (COV = coefficient of variation):

20% COV on the load coefficients

64% COV on N in the S-N curve (54% COV on $\ln N$)
 20% COV on Δ (damage at failure)

In the failure criterion for a time period T

$$\Delta - D = \Delta - \sum_{\theta} \sum_{(H_S, T_Z)} p_i q_j \frac{T}{K} (2\sqrt{2})^3 \nu_{0,ij} \text{Var}[\sigma_{ij}]^{3/2} \Gamma(1+3/2) \leq 0 \quad (3.9)$$

a (large) number of random variables are introduced. For each value of T the failure probability P_f , i.e., $P(\Delta - D \leq 0)$, is computed. First-order reliability method (FORM) are applied [1], and results are shown in Figure 3.4.

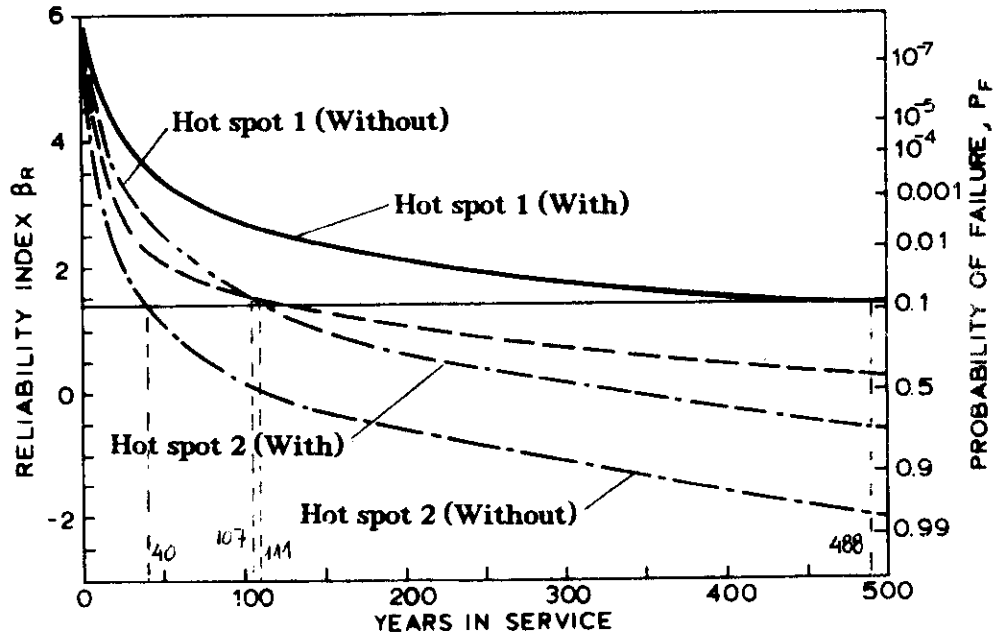


Figure 3.4 Reliability index β_R for hot spot 1 and 2 as function of years in service based on fracture mechanics.

The results are expressed in terms of a reliability index β_R which is uniquely related to the failure probability as

$$\beta_R = -\Phi^{-1}(P_f) \quad (3.10)$$

where $\Phi(\cdot)$ is the standard normal cumulative distribution function. Both the S-N curves in (3.5) and (3.6) are used. For the T-curve (3.5) the reliability index is approximately 1.4 for the deterministic life time of 488 years for hot spot 1 and also 1.4 for the deterministic life time 107 years for hot spot 2. For the S-N curve (3.6) the reliability index is also approximately 1.4 for the deterministic life time of 111 years of hot spot 1 and for the deterministic life time of 40 years for hot spot 2. This level $\beta \approx 1.4$ thus represent the level implicit in the technical standard for fatigue analysis with a requirement of the Miner sum ≤ 1 . The level is, however, not only linked to the technical standard but also to the specific uncertainty modeling applied.

For a more strict requirement - Miner sum < 0.1 - for joints which can not be inspected or repaired a reliability index around 4.7 is determined. In analyses of other structures the reliability indices have been around 3.7 and 1.2 rather than 4.7 and 1.4. The reliability index values agree well with suggested levels for annual failure probabilities for static failures, e.g. in NKB [5]. No such targets have, however, been formally stated for offshore structures.

Besides failure probabilities, various additional information is obtained. The total uncertainty is divided between the different sources. For hot spot 1 and $T=100$ years the result is shown in Table 3.4 for the S-N curve (3.6).

Source of uncertainty	Importance
Environmental description	1 %
Load model	19 %
Stress analysis	13 %
Fatigue strength	60 %
Damage criterion	7 %

The major source of uncertainty thus arises from uncertainty in the S-N curve.

Parametric sensitivity factors express the change in the reliability index to a change in a statistical distribution parameter, or deterministic design parameter. For $T=100$ years the sensitivity factor for the COV of the load coefficients V_l is

$$\frac{\partial \beta_R}{\partial V_l} = -0.81 \quad (3.11.a)$$

A reduction in the COV from 20% to 10% thus leads to an increase in the reliability index of approximately

$$\Delta \beta_R \approx (-0.81) \cdot (-0.10) = 0.081 \quad (3.11.b)$$

Omission sensitivity factors give the relative error on the reliability index if one random variable is replaced by its median, i.e. if one source of uncertainty is neglected. For $T=100$ years the omission sensitivity factor for the uncertainty in the load coefficients is

$$\frac{\beta_R(\text{deterministic load coefficients})}{\beta_R(\text{random load coefficient})} = \frac{1}{\sqrt{1-0.203^2}} = 1.02 \quad (3.12.a)$$

The reliability index is thus overestimated by a factor of 1.02, if the uncertainty in the load coefficient is neglected. Using omission sensitivity factors, based on one representative analysis, all but the important sources of uncertainty can be disregarded in subsequent analysis. Utmost care must, however, be shown in disregarding uncertainties, if the design analysis is followed by subsequent updating.

The probabilistic analysis is more involved than the deterministic analysis. The two analyses, however, result in almost identical rankings of the criticality of different hot spots. In practical analysis of large structures a deterministic analysis is therefore recommended to be applied first. This allows a filtering and the identification of the least reliable hot spots for which the probabilistic analysis is performed.

In the introduction it was mentioned that a distinction between subjective and objective uncertainties (randomness and uncertainty) is sometimes made. Let \mathbf{Z}_1 denote the random variables describing randomness and \mathbf{Z}_2 denote those describing uncertainty. The failure criterion as in Eq.(3.9) is written in terms of a limit state function $g(\cdot)$ as

$$g(\mathbf{Z}) = g(\mathbf{Z}_1, \mathbf{Z}_2) \leq 0 \tag{3.12.b}$$

and the failure probability P_F is computed as

$$\begin{aligned} P_F &= P(g(\mathbf{Z}) \leq 0) = P(g(\mathbf{Z}_1, \mathbf{Z}_2) \leq 0) \tag{3.12.c} \\ &= \int_{\mathbf{z}_2} P(g(\mathbf{Z}_1, \mathbf{z}_2) \leq 0) f_{\mathbf{z}_2}(\mathbf{z}_2) d\mathbf{z}_2 \\ &= \int_{\mathbf{z}_2} P_F(\mathbf{z}_2) f_{\mathbf{z}_2}(\mathbf{z}_2) d\mathbf{z}_2 = E[P_F(\mathbf{Z}_2)] \end{aligned}$$

$P_F(\mathbf{Z}_2)$ is a conditional failure probability and instead of only plotting the expected value $E[P_F(\mathbf{Z}_2)]$ one may plot curves corresponding to different fractiles, see Fig. 3.5. The left hand curve in this figure is as Fig. 3.4 while the right hand figure illustrates the alternative presentation (no actual calculations have been performed). The curve marked 10% thus shows reliability indices for which there is a 10% probability that the reliability index is smaller considering the subjective uncertainties.

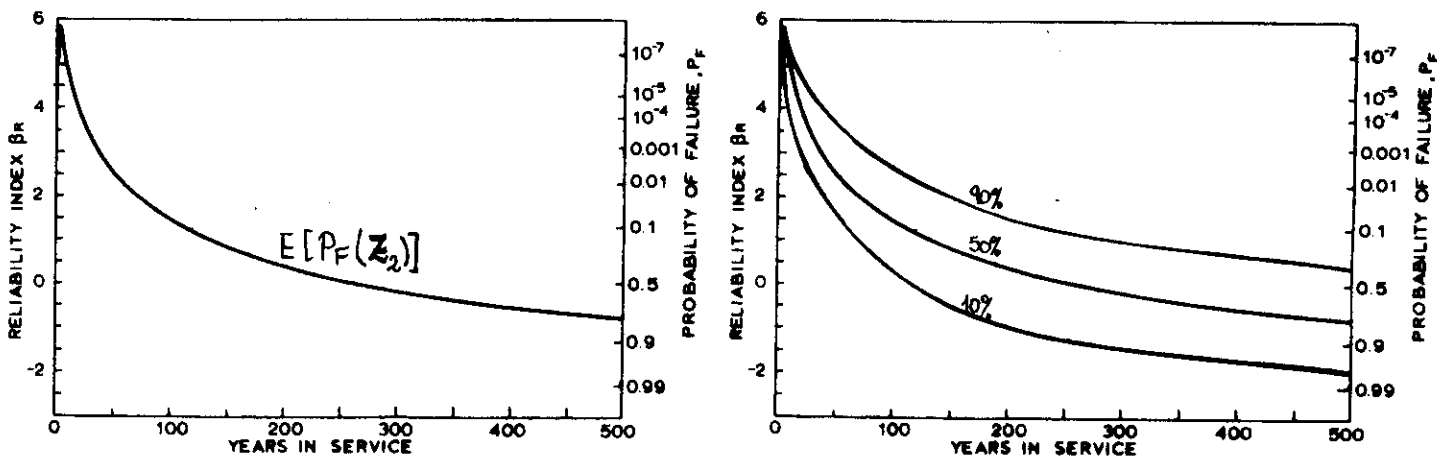


Figure 3.5 Alternative treatments of subjective probabilities in reliability index calculation.

The presentation on the right hand side in Fig. 3.5 may be judged as more informative than that on the left hand side as the importance of the subjective input is

better presented. In classical decision analysis with the objective to optimize the expected utility (e.g. minimize the total expected cost) only the expected value $E[P_F(Z_2)]$, however, enters the calculations, which is the reason why only this number is generally determined.

Figure 3.4 presents for various time periods the probability of crack growth through the thickness before the end of the period. By varying the critical crack size it is also possible, for each point in time, to determine the cumulative distribution function of the crack size and by applying the sensitivity factors also the probability density function. This information is illustrated in principle in Fig. 3.6 (this figure does not show result from the actual analysis) where the hatched areas show the failure probability.

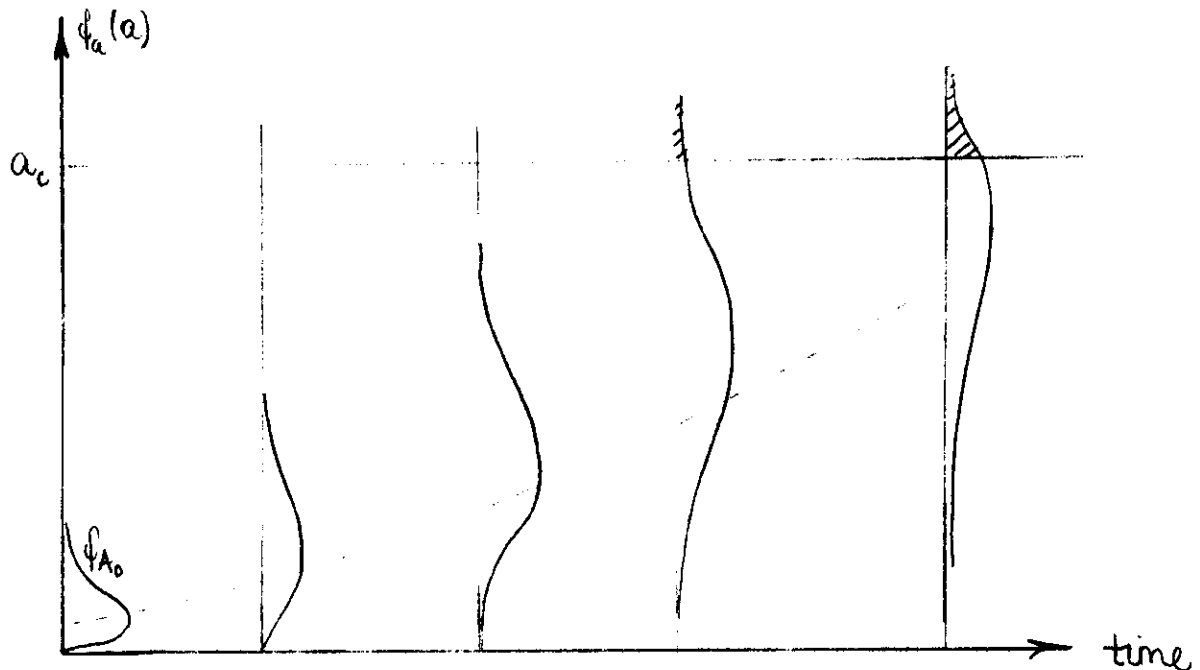


Figure 3.6 Probability density function for crack size at various times - dotted curve illustrates development of mean crack size.

3.3 Probabilistic fracture mechanics fatigue study

The probabilistic fracture mechanics study uses the same models for the environmental description, loading, global response and stress analysis as the probabilistic S-N fatigue analysis. The fatigue strength is, however, determined from a fracture mechanical description of crack growth from an initial size and through the thickness. A semi-elliptical surface crack is considered with depth a and length $2c$. A constant aspect ratio $a/c=0.15$ is assumed and the crack growth can be described in terms on the depth a . It is a straightforward generalization to describe the growth in both depth and length.

In a linear elastic fracture mechanics approach the increment in crack size, Δa , during a load cycle is related to the range of the stress intensity factor, ΔK , for the stress cycle. For a crack of length a , growing in an alternating elastic stress field of magnitude $\sigma(t)$, the increment of crack length for one cycle, Δa , is given by the Paris and Erdogan relationship

$$\frac{da}{dN} = C (\Delta K)^m, \quad \Delta K > \Delta K_{thr} = 0 \quad (3.13)$$

where C and m are functions of the material and environment and N is the number of stress cycles. The cyclic crack tip stress intensity range ΔK can be described by the following relationship

$$\Delta K = \Delta \sigma Y(a) \sqrt{\pi a} \quad (3.14)$$

where $\Delta \sigma$ is some indicator of the magnitude of the stress range (in the absence of the crack) and $Y(a)$ is a factor to allow for the crack and component geometry and the stress distribution over the crack. $Y(a)$ is here referred to as the geometry function. The crack growth equation can be extended to include a positive threshold ΔK_{thr} . For stress intensity factors ranges below the threshold value no crack growth takes place. More complicated relations than the linear $\log da/dN - \log \Delta K$ relation may also be introduced, when certain assumptions about the loading history are made. This aspect is, however, beyond the scope of this report.

The determination of the stress intensity factor requires a knowledge of the stress distribution σ through the wall thickness on the plane normal to the crack or assumed crack at the hot spot and along the circumferential direction. Here, σ is taken as the hot spot stress, i.e. the nominal stress multiplied by the global stress concentration factor (the same as used in the S-N fatigue analysis). The stress is computed for both axial, in-plane and out-of plane loading and added. The resulting stress through the thickness consists of a bending and a membrane component. Even under nominally axial loading, the stress in the through-thickness direction in a tubular joint is predominantly bending. For the actual unstiffened joint and hot spots the ratio between the local membrane and bending stresses is assumed to be 0.20 which is reasonable for the present tubular joint and crack location. This ratio is constant in this approximation. For a stiffened joint a larger ratio is typically found.

By using the simple formula for a surface crack in a flat plate acting under tension and bending [7], the $Y(a)$ factor for the actual hot spots can be estimated. The formulae for calculating the stress intensities for semi-elliptic cracks given in [7] were derived for linear stress fields (i.e. pure tension and pure bending). In welded joints, considerations must also be given to the non-linear stress fields arising from local stress concentrations at the weld toe. These have been modeled using a stress intensity multiplication factor M_k derived from finite element analysis, [8]. Two-dimensional models of welded joints were analysed with emphasis on the effect of small variations in the geometry of such models. This information was used to come up with an analytical form of the M_k solutions.

In addition to the effects of weld toe stress concentration and mixed bending - tension stresses, the stress distribution in the circumferential direction is varying. Therefore, the stress field at the tip of a surface crack will vary as the crack lengthens. The stress variations in the circumferential direction are not accounted for as constant hot spot stresses over the cracked region are applied here.

For the actual hot spots the factor $Y(a)$ is found to be (as a function of the thickness t)

$$Y(a) = Y_{unwelded}(a) \cdot M_k(a) \quad (3.15a)$$

$$Y_{unwelded}(a) = \left[1.08 - 0.70\left(\frac{a}{t}\right) \right] \quad (3.15b)$$

$$M_k(a) = \left[1.0 + 1.24 \cdot e^{-22.1\left(\frac{a}{t}\right)} + 3.17 \cdot e^{-357\left(\frac{a}{t}\right)} \right] \quad (3.15c)$$

The effective geometry function is shown in Figure 3.7.

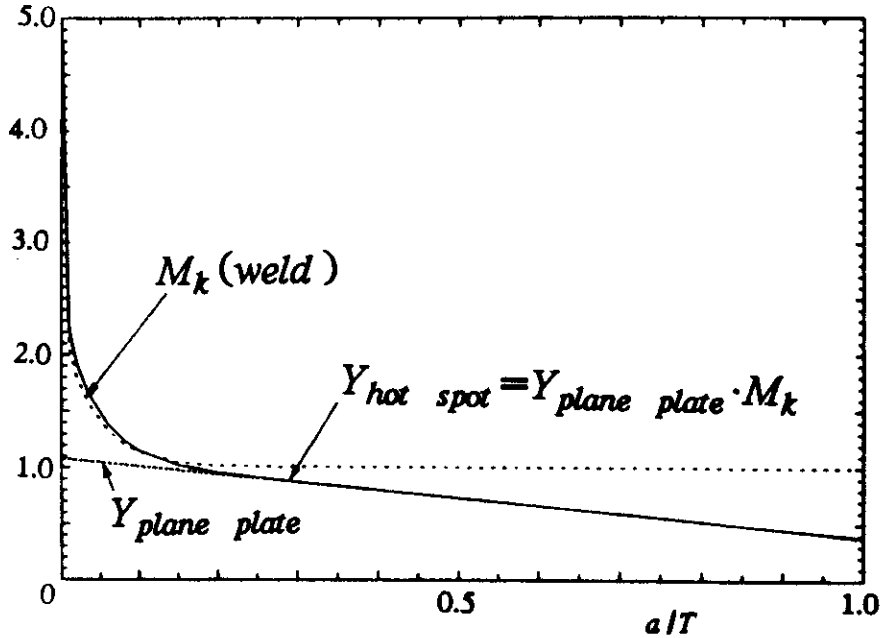


Figure 3.7 Geometry function for hot spot 1 and 2.

Integrating the crack growth equation (3.13) gives, see Appendix,

$$\int_{a_0}^a \frac{dx}{Y(x)^m (\pi x)^{m/2}} = C \sum_{i=1}^N S_i^m \quad (3.16)$$

where a_0 is the initial crack depth and a is the crack depth after N stress cycles. Stress ranges are denoted by S_i . An initial period of time before the crack starts growing can be included either by introducing a crack initiation period or applying an equivalent flaw size distribution. For a welded offshore joint the crack initiation period is generally small and this certainly applies to joints which fail during the

service life.

With failure corresponding to crack growth through the thickness, the failure criterion becomes

$$\int_{a_0}^{a_c} \frac{dx}{Y(x)^m (\pi x)^{m/2}} - C \sum_{i=1}^N S_i^m \leq 0 \quad (3.17)$$

The safety margin M is therefore defined as

$$M = \int_{a_0}^{a_c} \frac{dx}{Y(x)^m (\pi x)^{m/2}} - C \sum_{i=1}^N S_i^m \quad (3.18)$$

and the failure probability P_F is

$$P_F = P(M \leq 0) \quad (3.19)$$

For constant amplitude loading with stress range S the relation between S and the number of cycles to failure is determined as

$$N = \frac{1}{C} \int_{a_0}^{a_c} \frac{dx}{Y(x)^m (\pi x)^{m/2}} S^{-m} = \text{constant} \cdot S^{-m} \quad (3.20)$$

i.e. the same form as (3.6). A measure of damage can be defined as

$$D = \frac{\int_{a_0}^a \frac{dx}{Y(x)^m (\pi x)^{m/2}}}{\int_{a_0}^{a_c} \frac{dx}{Y(x)^m (\pi x)^{m/2}}} \quad (3.21)$$

This damage measure increases from an initial value 0 to 1. The increment in D from a stress cycle of range S_i is

$$\Delta D_i = \frac{\Delta \left(\int_{a_0}^a \frac{dx}{Y(x)^m (\pi x)^{m/2}} \right)}{\int_{a_0}^{a_c} \frac{dx}{Y(x)^m (\pi x)^{m/2}}} = \frac{C S_i^m}{N(S_i) C S_i^m} = \frac{1}{N(S_i)} \quad (3.22)$$

i.e. of the same form as (3.7). The S-N fatigue analysis and the fracture mechanics analysis are thus equivalent methods in the failure analysis.

In addition to the random variables is the load model, random variables are introduced for the initial crack size, parameters in the geometry function, and material parameters. An exponential distribution with a mean value 0.11 mm is used for a_0 as suggested in [9]. The geometry function (3.15a) is randomized by multiplying the expression with a random variable which is lognormal distributed with mean value 1.0 and COV 10 %. A fixed value of $m=3$ is used and the COV on

$\ln C$ is taken as 50%, together with a mean value of -29.75 on $\ln C$ (units N,mm). The data on C are not unrealistic but are on the other hand not very well documented. They have been selected to give good correspondence between the S-N analysis and the fracture mechanics analysis. The mean value of C differs by 10% from the value suggested in DnV [10] and the coefficient of variation agrees well with values proposed elsewhere.

Figure 3.8 shows similarly to Figure 3.4 results of a FORM analysis for the failure criterion in (3.18) for hot spot 1 and hot spot 2. Figure 3.9 combines the results of Figs. 3.4 and 3.8 and almost identical results are observed.

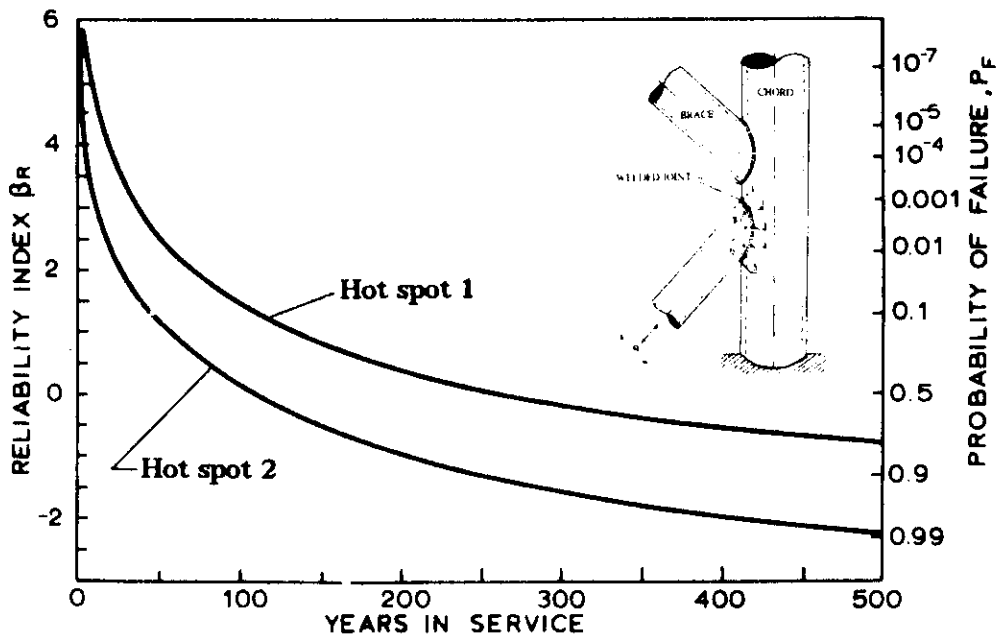


Figure 3.8 FORM results - probabilistic fracture mechanics fatigue study.

Importance factors similar to those of Table 3.4 are presented for $T=100$ years in Table 3.5. The major part of uncertainty is thus from the material parameter C .

3.4 Effect of inspection procedures

The updating based on inspection results can be performed with the stress range distribution resulting from the detailed uncertainty modeling of the environmental conditions, load model, global response and stress calculation. It is, however, extremely time saving to calibrate a stress range distribution with a smaller number of random variables. A Weibull distribution is selected

$$F_S(s) = 1 - \exp \left[- \left(\frac{s}{A} \right)^B \right], \quad s > 0 \quad (3.23)$$

A and B are random distribution parameters which are calibrated to include the uncertainties described above. A joint normal distribution for $(\ln A, 1/B)$ is selected.

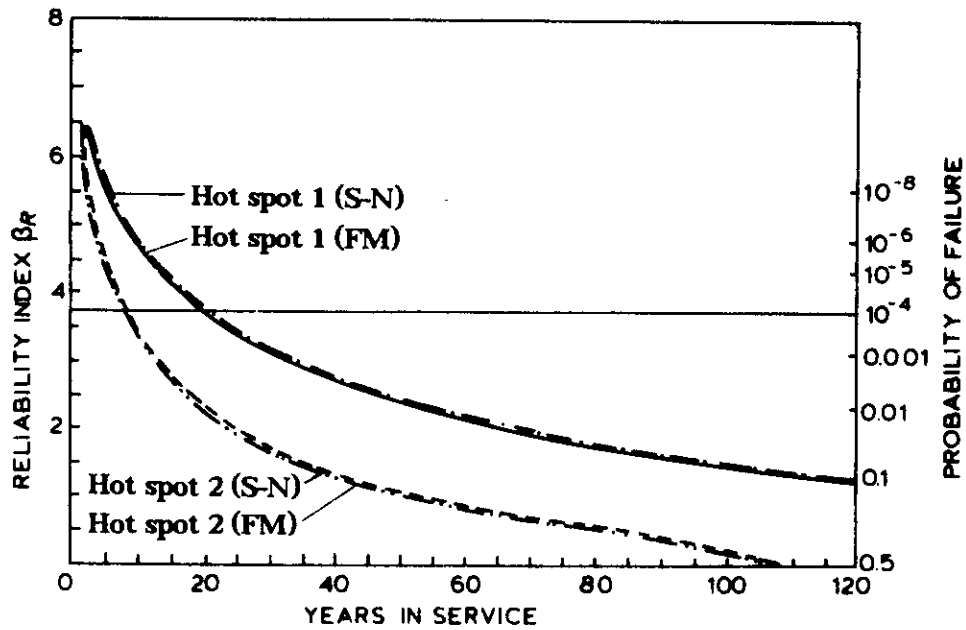


Figure 3.9 Comparison - probabilistic S-N fatigue analysis and probabilistic fracture mechanics fatigue analysis.

Table 3.5		Importance factors
Source of uncertainty	Importance	
Environmental description	1 %	
Load model	19 %	
Stress analysis	20 %	
Stress intensity factor	10 %	
Crack growth parameters	50 %	

The procedure is based on a first-order reliability analysis for selected fractiles in the long term distribution of stress ranges and the following results are obtained:

$$E[\ln A] = 1.60, \sigma[\ln A] = 0.22, E[1/B] = 1.31, \sigma[1/B] = 0.14, \rho[\ln A, 1/B] = -0.79$$

Figure 3.10 shows the comparison between the results from the original and the simplified stress range distribution. A very close agreement is observed.

With the simplified stress distribution, the sum in the safety margin (3.18) is replaced by

$$\sum_{i=1}^N S_i^m = N A^m \Gamma(1 + \frac{m}{B}) \tag{3.24}$$

where N is the total number of stress cycles which is determined from the same calibration procedure.

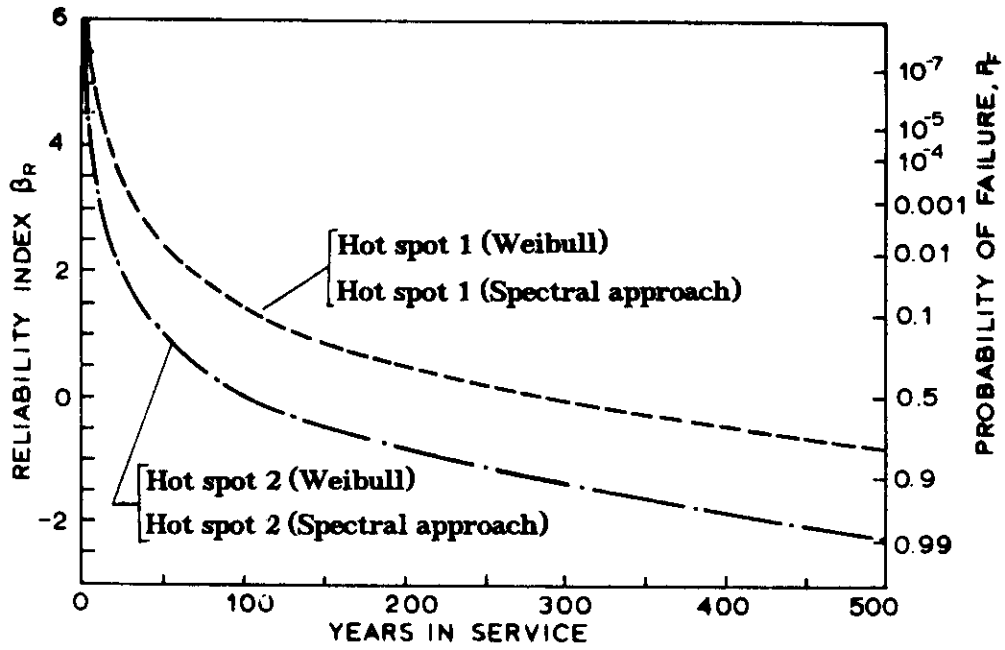


Figure 3.10 Comparison probabilistic fracture mechanics study - detailed and simplified stress range distribution uncertainty.

In-service inspection is performed in order to assure that the existing cracks in the structure which may be present from the initial delivery or arise at a later stage during the service time do not grow to critical sizes. The result from an inspection is either no detection or detection of a crack, i.e.,

$$a(T_i) \leq A_{di} \tag{3.25}$$

$$a(T_j) = A_j \tag{3.26}$$

In the first case, (3.25), no crack was found in the inspection after the time T_i , implying that the crack size was smaller than the smallest detectable crack size A_{di} . A_{di} is obviously a random variable, since a detectable crack is only detected with a certain probability. The distribution function for A_{di} is equal to the probability of detection function and here taken as (2.1). When more inspections are performed the random variables A_{di} are assumed mutually independent. In the second case, (3.26), a crack size A_j is observed after the time T_j . A_j is also random due to measurement error and/or due to uncertainties in the interpretation of a measured signal as a crack size.

For each inspection which results in no crack detection (3.25) an event margin M_i can be defined similar to the safety margin (3.18) as

$$M_i = CN_i A^m \Gamma\left(1 + \frac{m}{B}\right) - \int_{a_0}^{A_{di}} \frac{dx}{Y(x)^m (\pi x)^{m/2}} \leq 0, \quad i = 1, 2, \dots, r \tag{3.27}$$

These event margins are negative due to (3.25). For each measurement (3.26) an

event margin M_j can similarly be defined as

$$M_j = \int_{a_0}^{A_j} \frac{dx}{Y(x)^m (\pi x)^{m/2}} - CN_j A^m \Gamma(1 + \frac{m}{B}) = 0, \quad j=1,2,\dots,s \quad (3.28)$$

These event margins are zero due to (3.26). The situation where a crack is not detected in r inspections at a location is now considered. The updated failure probability P_F^u is in this case

$$P_F^u = P(M \leq 0 | M_1 \leq 0 \cap M_2 \leq 0 \cap \dots \cap M_r \leq 0) \quad (3.29)$$

This expression can be calculated by solving the FORM problem for two parallel systems, one for the numerator and one for the denominator, respectively, of the expression

$$P_F^u = \frac{P(M \leq 0 \cap M_1 \leq 0 \cap \dots \cap M_r \leq 0)}{P(M_1 \leq 0 \cap \dots \cap M_r \leq 0)} \quad (3.30)$$

The situation where cracks are found in an inspection can be described as a direct generalization. For more details see the Appendix.

Assuming that a repair takes place after N_{rep} stress cycles and a crack a_{rep} is observed, an event margin M_{rep} is defined as

$$M_{rep} = \int_{a_0}^{a_{rep}} \frac{dx}{Y(x)^m (\pi x)^{m/2}} - ACN_{rep} A^m \Gamma(1 + \frac{m}{B}) = 0 \quad (3.31)$$

The crack size present after repair and a possible inspection is a random variable a_{new} and the material properties after repair are m_{new} and C_{new} . The safety margin after repair is M_{new}

$$M_{new} = \int_{a_{new}}^{a_C} \frac{dx}{Y(x)^{m_{new}} (\pi x)^{m_{new}/2}} - C_{new} (N - N_{rep}) A^{m_{new}} \Gamma(1 + \frac{m_{new}}{B}) \quad (3.32)$$

and the updated failure probability after repair is

$$P_F^u = P(M_{new} \leq 0 | M_{rep} = 0) \quad (3.33)$$

This updated failure probability is then of the same form as for (3.29).

To illustrate the effect of an inspection which does not lead to crack detection Fig.3.11 has been prepared. The probability density function for the crack size before the inspection is $f_a(a)$ and after the inspection $f'_a(a)$. These are related by

$$f'_a(a) = \frac{f_a(a)(1-P_d(a))}{\int_0^\infty f_a(a)(1-P_d(a))da} \quad (3.34)$$

$f_a(a)$, the probability of not detecting a crack of size a $1-P_d(a)$, and $f'_a(a)$ are shown in Fig.3.11. Figure 3.12 shows a development with several inspections and no crack detection and Fig.3.13 a development with a crack detection and no repair

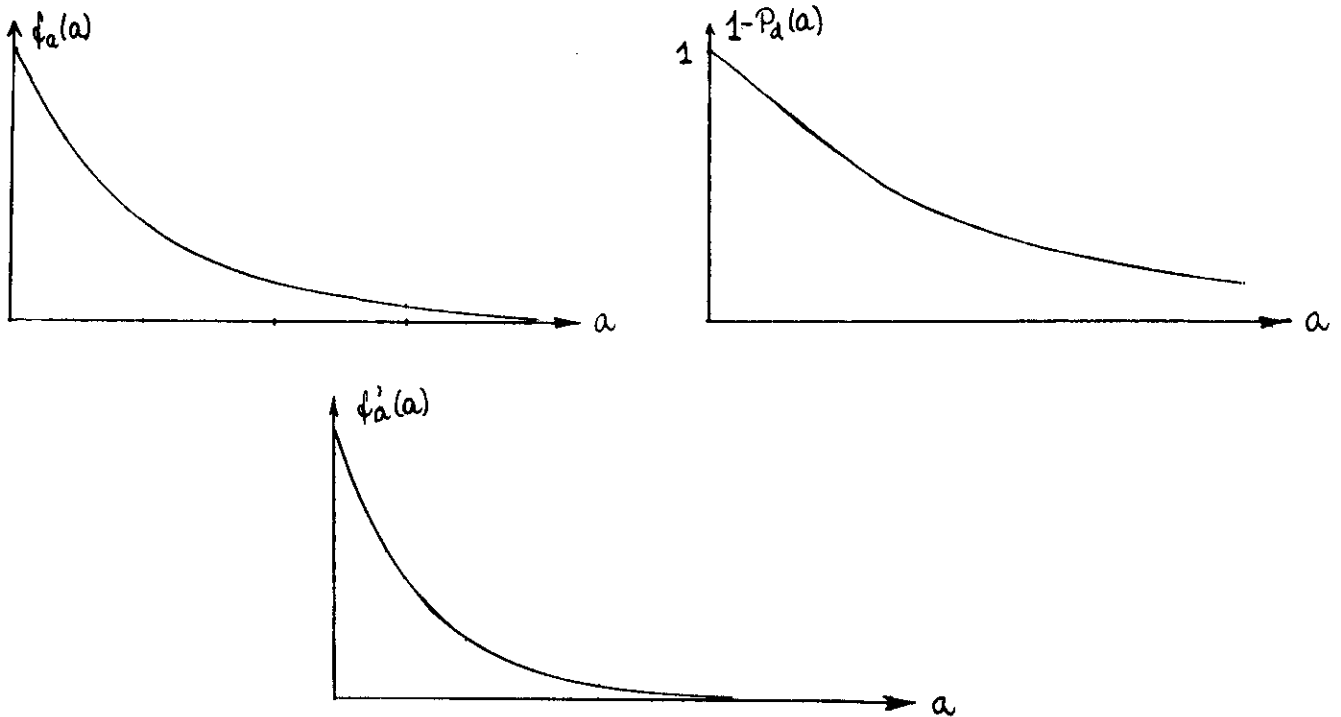


Figure 3.11 Updating of probability density function of crack size when no crack is detected.

and a crack detection and repair (none of these figures show results of actual calculations).

The effect of MPI on the reliability of hot spot 1 which has an deterministic life time of 111 years, Table 3.3, is considered. The design life time is taken as 100 years. The time of the first inspection is selected such that the probability of failure before this time is 10^{-4} corresponding to a reliability index $\beta=3.72$, i.e. after 20 years according to Fig.3.14.a. This probability level is not stated in any offshore code as a requirement but is here selected as a number which appears appropriate. The general conclusions are not very dependent on the number, but clearly the resulting number of inspections depends on it. The choice of $\beta=4.7$ could also be considered as this corresponds to the reliability index inherent in the code when inspection and repair is not possible and the design must have a Miner sum less than 0.1.

It is assumed that no crack is detected in the first inspection. The reliability is then updated according to Eq.(3.30) as shown in Fig.3.14.b. The solid reliability index curve in this figure corresponds to failure before the considered time. To avoid confusion, it must however be emphasized that the two parts of the curve are not based on the same information. The figure does therefore not show a cumulative distribution function for the fatigue life time derived before the inspection program starts (such a cumulative distribution function is monotonic). The reliability index just after the inspection at 20 years corresponds to the probability that failure has occurred (the crack has grown through the thickness) but this is not detected.

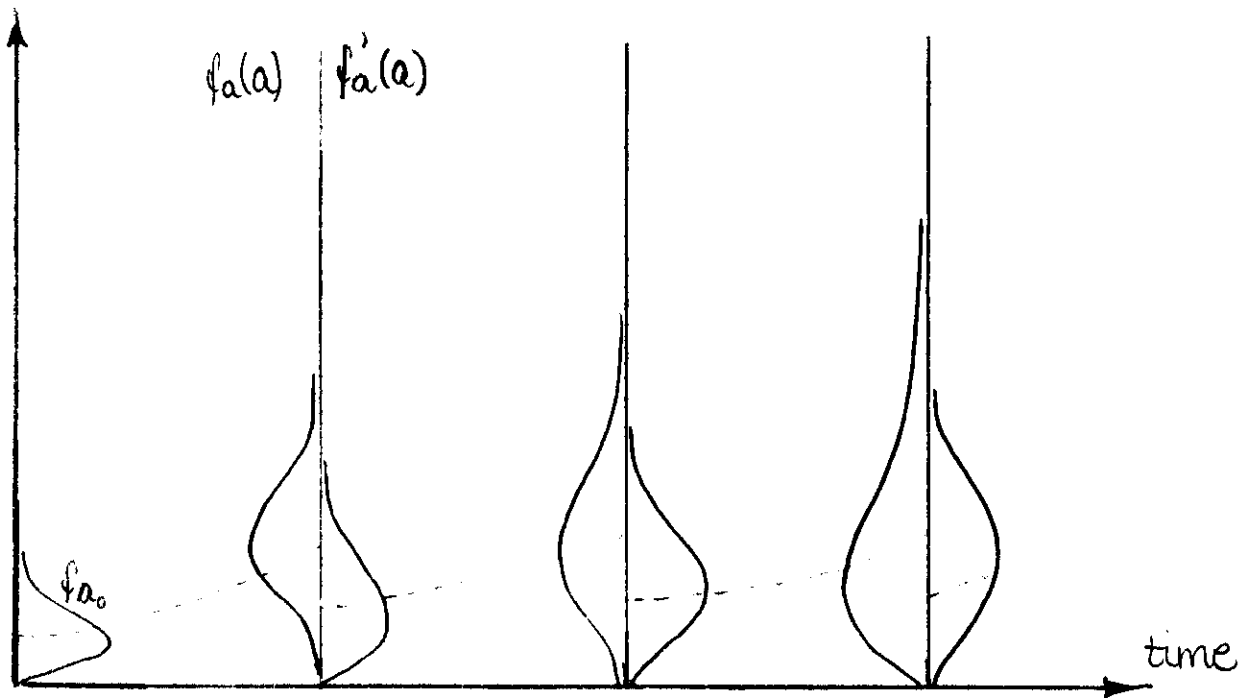


Figure 3.12 Updating of crack size density function when no crack is detected in several successive inspections.

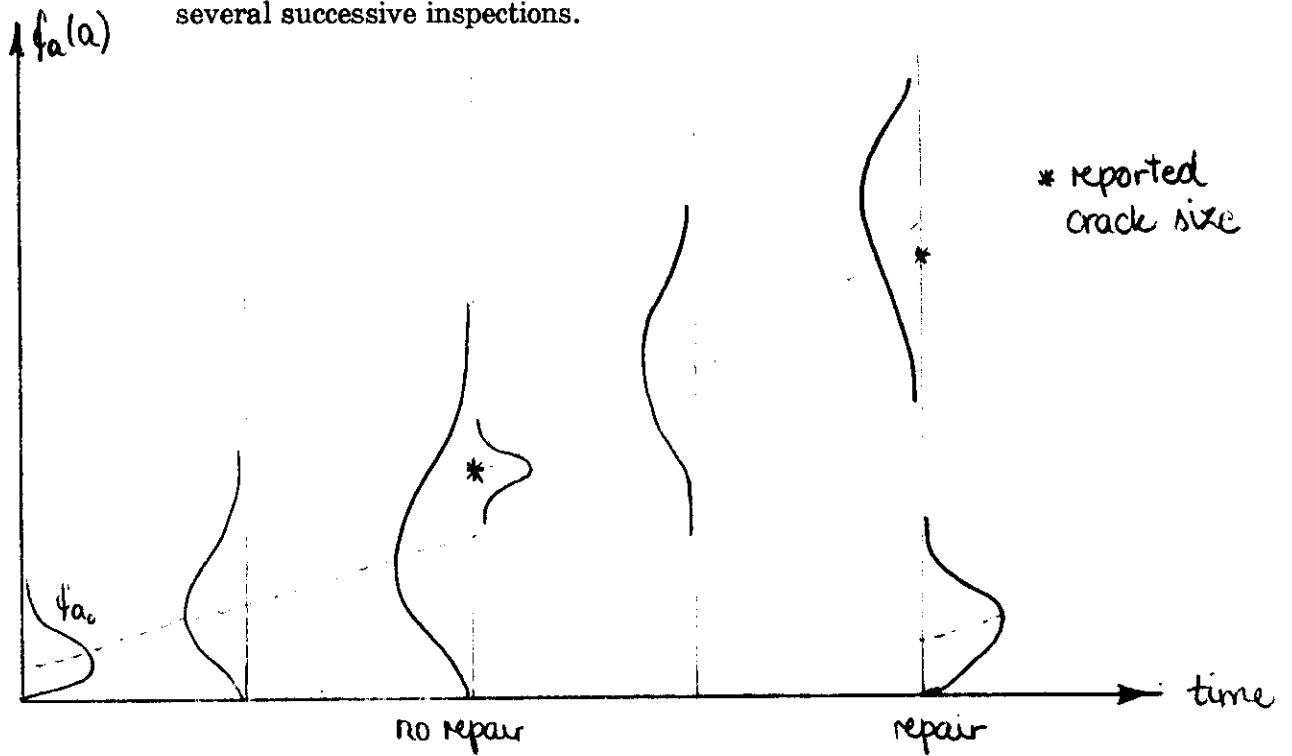


Figure 3.13 Updating of crack size density function when a crack is detected and measured, not repaired or repaired.

After the first inspection the reliability index decreases with time as shown in Figure 3.14.c where the development for fixed inspection intervals of 20 years is shown. The updated reliability level is above $\beta_R^u = 3.72$ or the updated probability of failure P_F^u is below 10^{-4} throughout the life time of 100 years. Figure 3.15 shows the same results as Fig.3.14 but for another assumed quality of MPI inspection (another POD curve given in Eq.(2.1)).

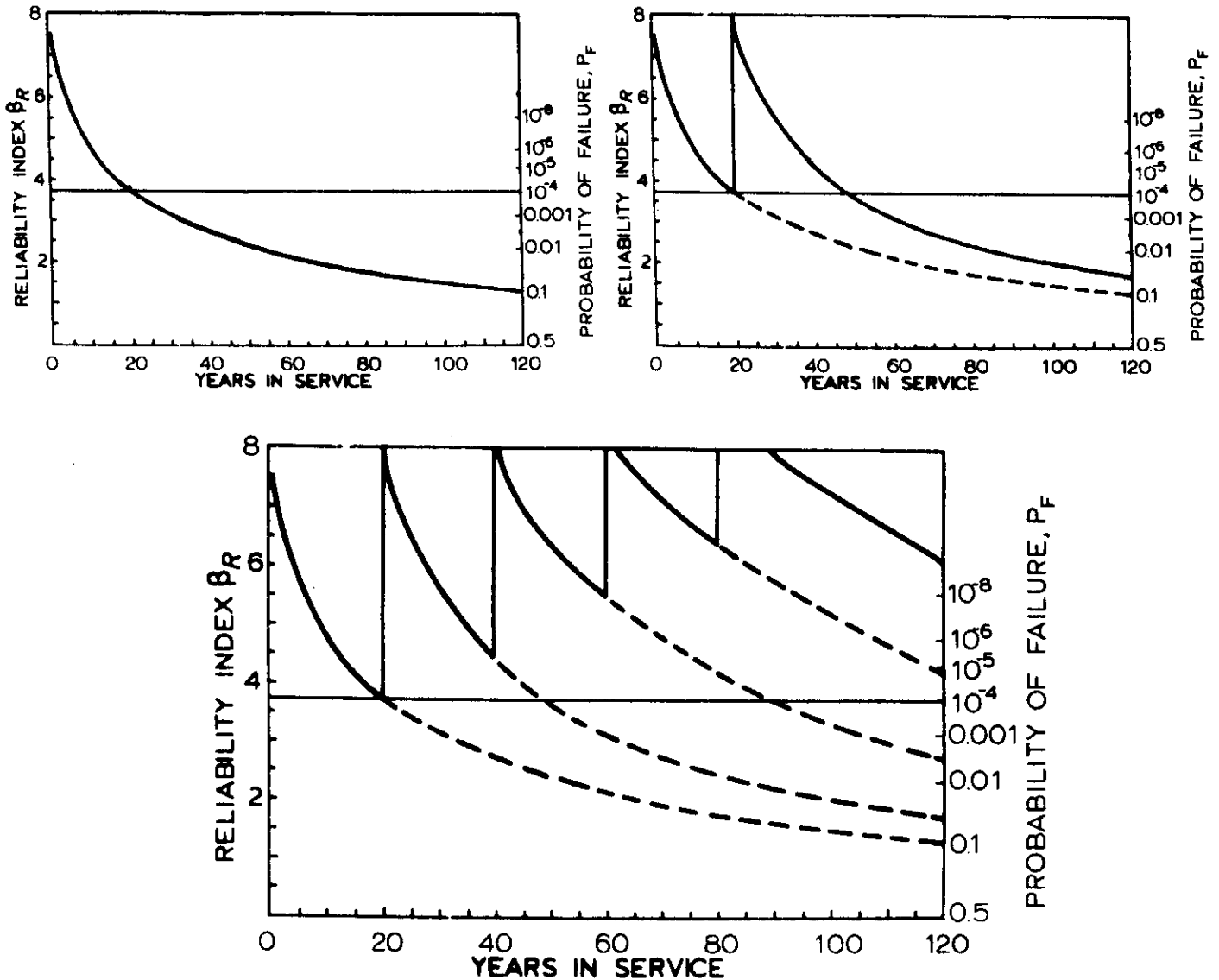


Figure 3.14 Updated first-order reliability index after inspections with MPI with no crack detection. Regular intervals, $\lambda = 1.3$ mm in POD curve Eq.(2.1).

Figures 3.16 and 3.17 show for the two MPI POD-curves the necessary amount of inspection to achieve a level above $\beta_R = 3.72$. It is observed that only two inspections respectively three inspections are needed. A potential reduction of 50 % and 25 % respectively is thus present.

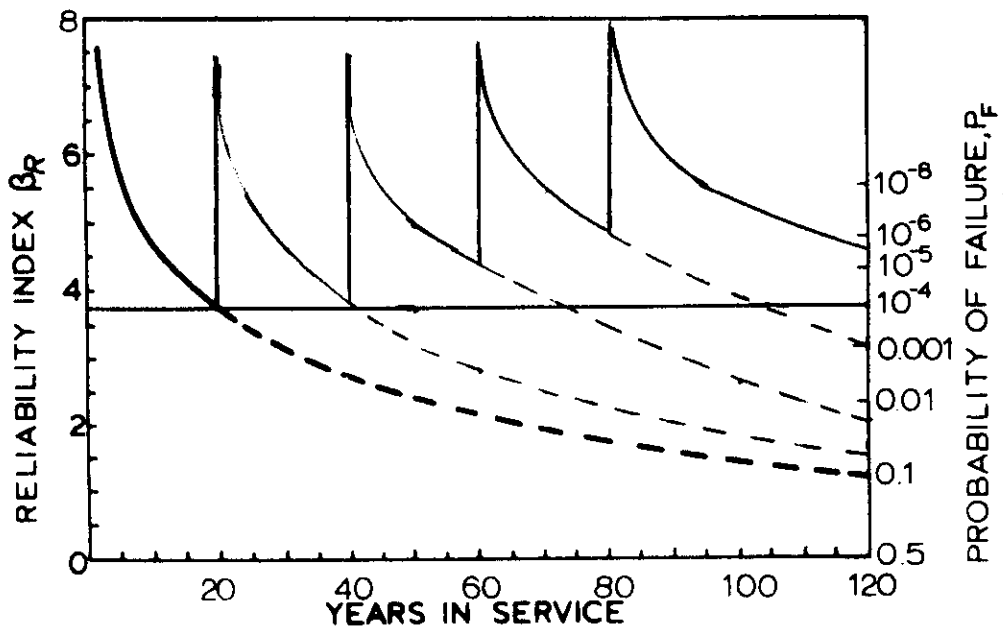


Figure 3.15 Updated first-order reliability index after inspections with MPI with no crack detection. Regular intervals, $\lambda = 2.6$ mm in POD curve Eq.(2.1).

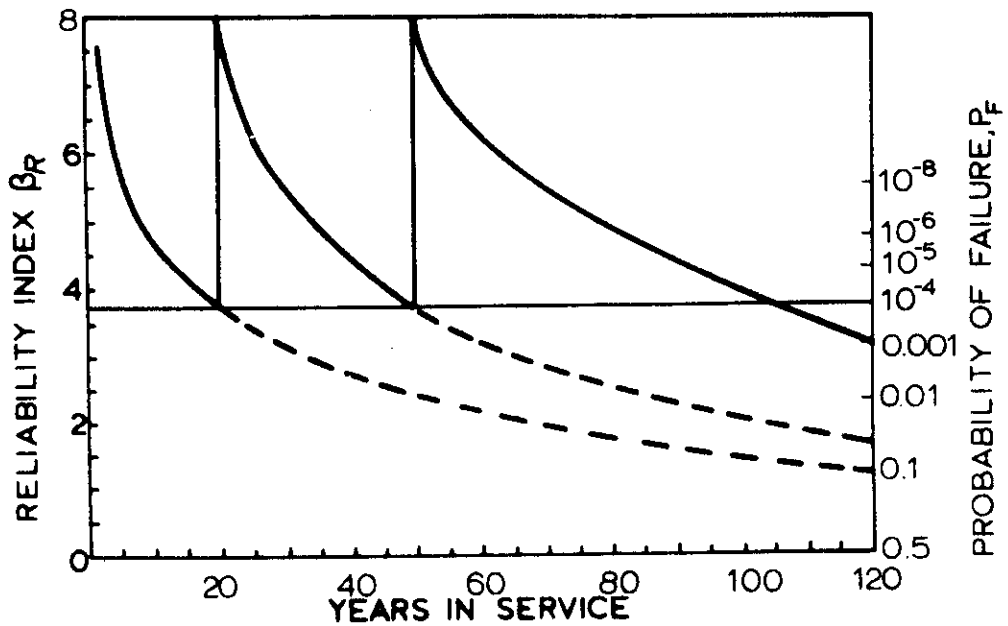


Figure 3.16 Updated first-order reliability index when the MPI inspections are optimized. $\lambda = 1.3$ mm in POD curve Eq.(2.1).

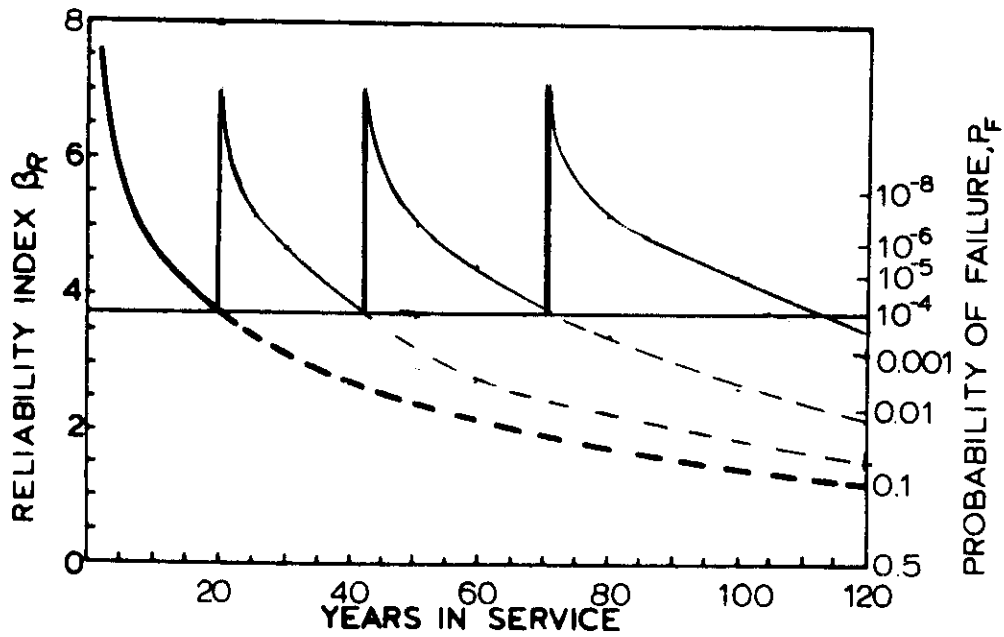


Figure 3.17 Updated first-order reliability index when the MPI inspections are optimized. $\lambda = 2.6$ mm in POD curve Eq.(2.1).

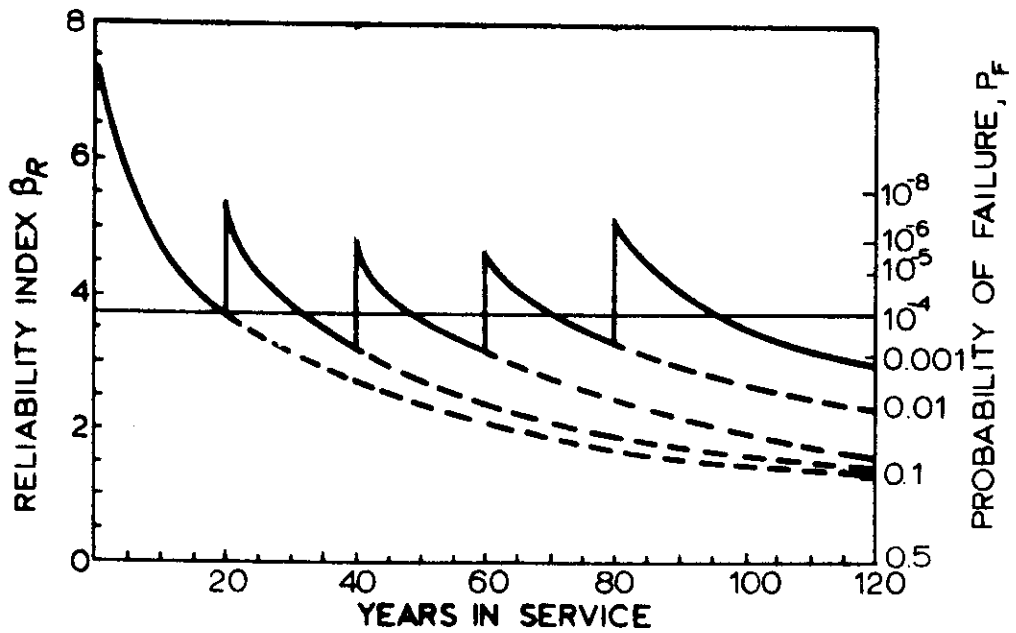


Figure 3.18 Updated first-order reliability index after visual inspection with no crack detection. Regular intervals, $\lambda = 6.5$ mm in POD curve Eq.(2.1).

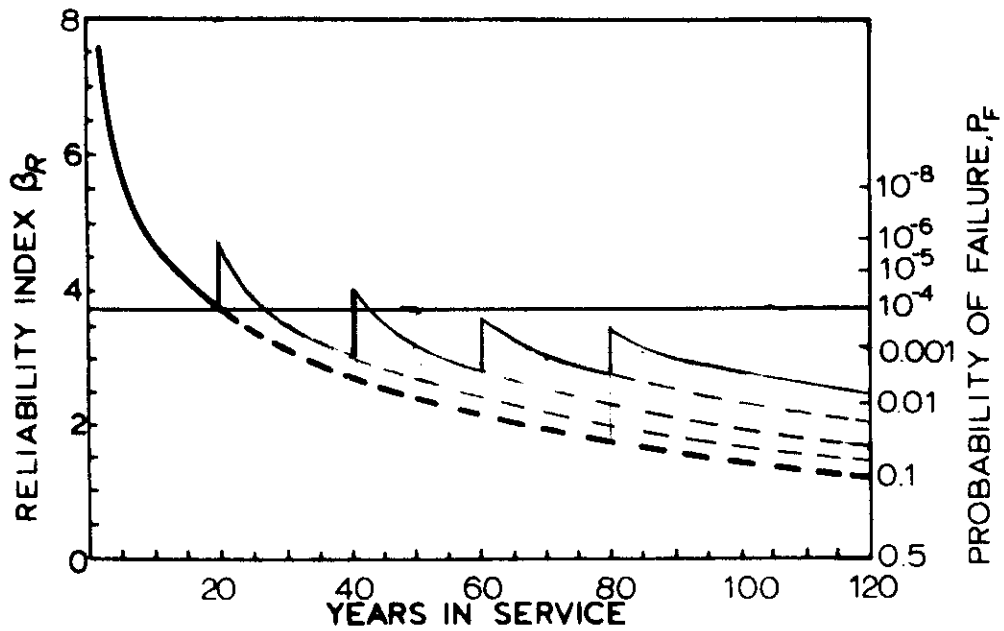


Figure 3.19 Updated first-order reliability index after visual inspections with no crack detection. Regular intervals, $\lambda = 13.0$ mm in POD curve Eq.(2.1).

For visual inspection Figures 3.18 and 3.19 show similarly to Figures 3.14 and 3.15 for MPI the reliability for an inspection strategy with inspection every 20th year. It is again assumed that no cracks are detected. The visual inspection is not able to maintain a reliability level above $\beta_R = 3.72$ throughout the life time, although the reliability level immediately before an inspection increases also in this case. To maintain a reliability level larger than 3.72 thus requires 5 respectively 10 inspections, see Figures 3.20 and 3.21.

When a crack is detected and the size is measured a decision must be made on whether or not to repair immediately. The analysis includes measurement uncertainty in sizing the detected crack - either directly or indirectly. With a criterion for the reliability between two inspections, a safe period of operation can be determined and a decision on repair be somewhat postponed. The situation in which a repair takes place and the reliability after repair is shown in Figure 3.22. It is assumed that a crack size of $a_{rep} = 4$ mm is repaired after 20 years. The distribution of the initial crack size after repair a_{new} is taken as an exponential distribution with a mean value of 0.11 mm, i.e. as the same initial distribution as after installation. Independent material properties are assumed in this case and the same distribution is used for the properties before and after repair. It follows from the results that there is an immediate increase in reliability after repair, but the reliability drops below the level obtained by the design calculations. This reflects the possibility that the cause for the repaired crack is a larger than anticipated loading of the hot spot, which is also acting after repair.

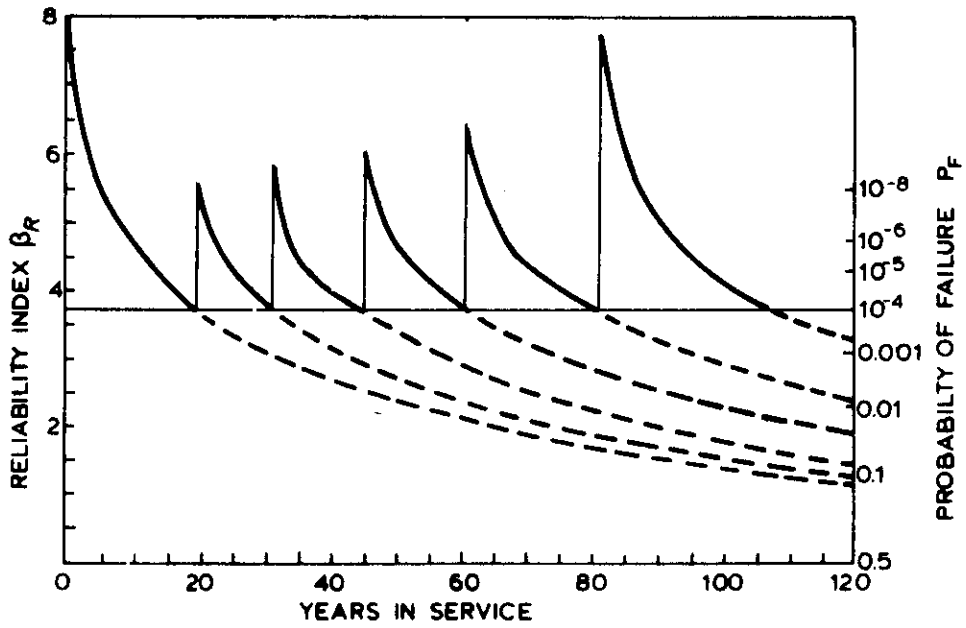


Figure 3.20 Updated first-order reliability index when the visual inspections are optimized. $\lambda = 6.5$ mm in POD curve Eq.(2.1).

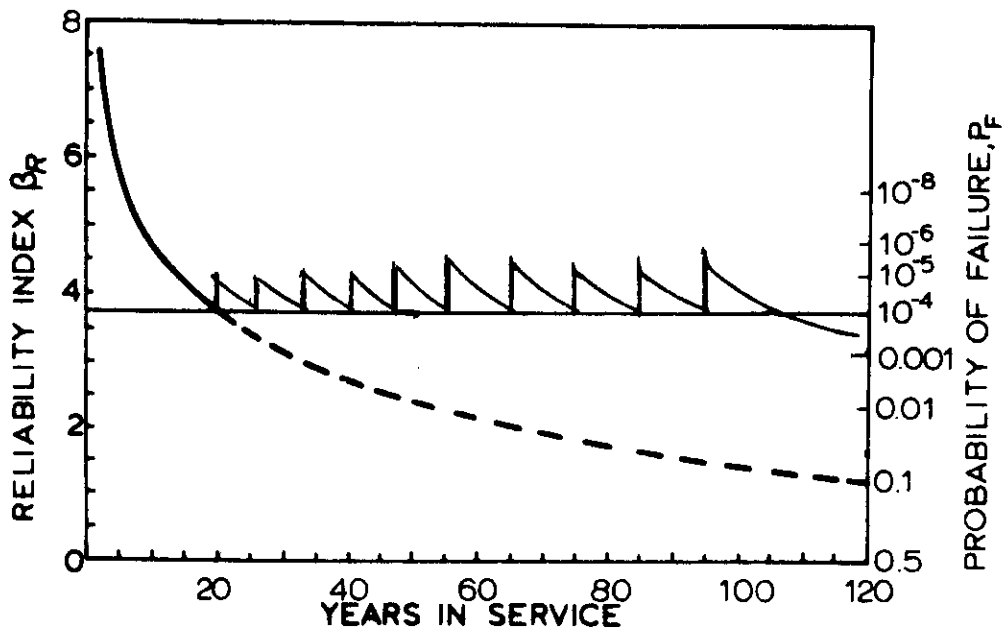


Figure 3.21 Updated first-order reliability index when the visual inspections are optimized. $\lambda = 13.0$ mm in POD curve Eq.(2.1).

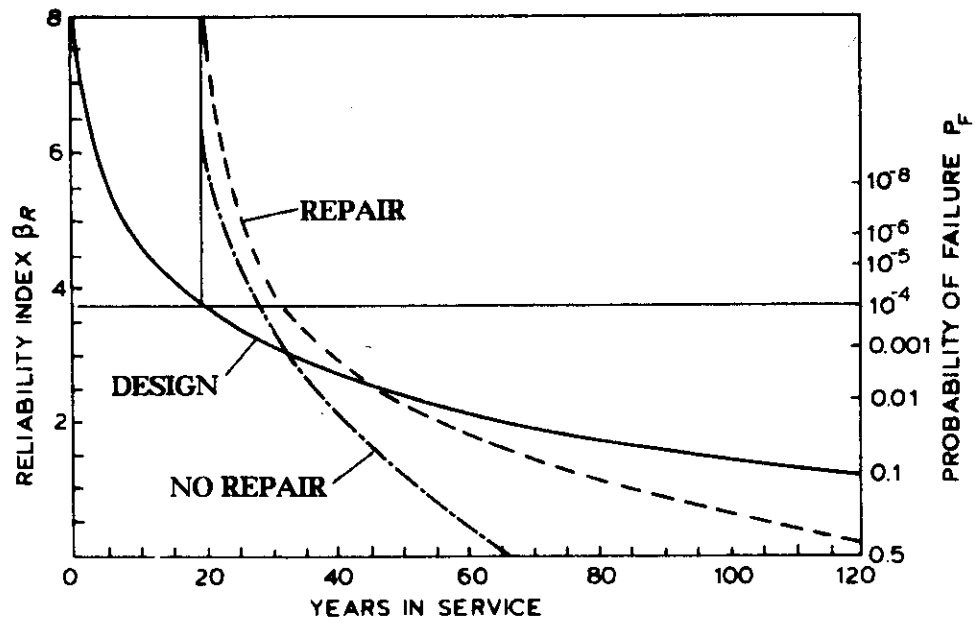


Figure 3.22 Updated first-order reliability index after repair of an 4 mm crack after 20 years.

4. APPRAISAL OF THE LIMITATIONS OF THE ANALYSIS.

The limitations in terms of modeling capabilities and available data are discussed. Some of these limitations are of fundamental nature while others may be removed, however, often at significant cost. The models applied in the analysis represent a compromise between easy use and accurate description of real world performance. With the improvements suggested below the models are, however, very well suited in decision making concerning inspection planning and repair. Already with the present state of the methods their use can be very beneficial, i.e. the reliability can be improved for a fixed inspection budget or the inspection costs can be reduced while maintaining the reliability.

Models for environmental conditions, load models, global structural analysis models, and local stress analysis models applied in the analysis are well accepted and verified. Good estimates for the mean values of input parameters are generally available. Through many studies in recent years it is also possible to give sound estimates for the coefficients of variation. The distribution types have not been accurately assessed and formal choices must be made.

In computing stress intensity factors the analysis presented here applies a simplified approach. With forthcoming finite element codes for cracked joints this computation may soon be improved at a reasonable cost. When the only inspection consists in detection of leakage, an important phase in this context is where the crack grows through the thickness and starts a circumferential growth. No good knowledge of stress intensity factors are presently available for this phase. The problem is, however, equally critical for deterministic as for probabilistic calculations.

The Paris and Erdogan equation for crack growth is adopted and no interaction effects are included, i.e., the order in which the load cycles appear is considered of no importance. A possible effect of the mean stress level including residual stresses is also excluded. These assumptions are made in almost all deterministic analyses, but are more fundamental for the success of the probabilistic analysis. Without these assumptions the variables in the differential equation cannot be separated and under variable amplitude loading not only the moments of stress range distributions are needed. When the assumptions are not valid simulation is the only available alternative to the analytical methods presented here. The computation time then becomes prohibitively long for a probabilistic analysis.

Data on initial defect sizes and the material parameters governing crack growth are sparse.

Acceptance criteria in probabilistic analyses need to be defined. This applies both to the design situation, but in particular to a situation with updating based on inspection results. No "safe" periods of operation without inspection/repair can otherwise be identified. A calibration to existing "acceptable" design practice is the easiest solution, but may break down for new design situations. An international standardization of distribution types for the uncertain parameters and of acceptance levels is being prepared on a long term basis.

Acceptance criteria for individual joints and members must reflect the consequences of failure in terms of reduction of system reliability. To this end system reliability methods - even in a simplified form - must be available. Although much

research work is carried out in this area no satisfactory system reliability analysis procedures have been devised. Good progress is, however, reported by many researchers.

REFERENCES

- [1] Madsen H.O., Krenk S. and Lind N.C. "*Methods of Structural Safety*" Prentice-Hall, Englewood Cliffs, New Jersey, 1986.
- [2] Gray A.M. "*The Reliability of Inspection Methods Applied to Marine Structures*" MSc Thesis: Cranford Institute of Technology, School of Industrial Science, 1986.
- [3] UK Department of Energy "*Remaining Life of Defective Tubular Joints - An Assessment based on Data for Surface Crack Growth in Tubular Joint Fatigue Tests*". Report No. 87-259, HMSO, London, 1987.
- [4] Skjong.R and Madsen H.O. "*Practical Stochastic Fatigue Analysis of Offshore Platforms*". Ocean Engineering, Vol.14, No.4, 1987, pp. 313-324.
- [5] UK Department of Energy, "*Offshore Installations: Guidance on design and construction*", HMSO, London, April, 1984.
- [6] NKB (The Nordic Committee on Building Regulations), "*Recommendations for Loading and Safety Regulations for Structural Design*", NKB-Report, Copenhagen, November 1978.
- [7] Raju I.S and Newman J.C "*An Empirical Stress-Intensity Factor Equation for Surface Crack*", Eng Frac. Mech, Vol 15, 1981, pp 185-192.
- [8] Smith I.J. and Hurworth S.J. "*The Effect of Geometry Changes upon the Predicted Fatigue Strength of Welded Joints*". Weld. Inst. Res. Report 244/1984. July, 1984
- [9] Bokalrud T. and Karlsen A. "*Probabilistic Fracture Mechanic Evaluation of Fatigue from Weld Defects in Butt Welded Joints*" Fitness for Purpose Validation of Welded Constructions, London 17-19 November 1981.
- [10] Det norske Veritas (DnV) "*Rules for the Design, Construction and Inspection of Offshore Structures, Appendix C Steel Structures*. Reprint with Corrections, 1982.

APPENDIX

PROBABILISTIC FATIGUE CRACK GROWTH ANALYSIS
OF OFFSHORE STRUCTURES, WITH RELIABILITY
UPDATING THROUGH INSPECTION

*Henrik O. Madsen*¹⁾, *Rolf Skjong*¹⁾,
*Andrew G. Tallin*²⁾, and *Finn Kirkemo*³⁾

ABSTRACT

A stochastic model for fatigue crack growth is applied, which accounts for uncertainties in loading, initial and critical defect sizes, material parameters including spatial variation, and in the uncertainty related to computation of the stress intensity factor. Failure probabilities are computed by first- and second-order reliability methods and sensitivity factors are determined. Model updating based on in-service inspection results is formulated within the first-order reliability method. Updated failure probabilities are computed and the distributions of the basic variables are updated. Two types of in-service inspection results are used to update the computed failure probabilities. Inspections which do not detect a crack are used and the inspection uncertainty is included in terms of the distribution of nondetected crack sizes by the specific inspection method. Inspections which detect a crack are also included and the inspection uncertainty is included through the uncertainty in the measured crack size. The formulations are presented for updating based on one or more inspections. A similar formulation for reliability updating after repair is provided within the same framework.

1. INTRODUCTION

In offshore steel structures flaws are inherent due to, e.g., notches, welding defects and voids. Macro cracks can originate from these flaws and under time varying loading grow to a critical size causing catastrophic failure. The conditions governing the fatigue crack growth are the geometry of the structure and crack initiation site, the material characteristics, the environmental conditions and the loading. In general, these conditions are of random nature. The appropriate analysis and design methodologies should therefore be based on probabilistic methods.

In recent years considerable research efforts have been reported on probabilistic modeling of fatigue crack growth based on a fracture mechanics approach, see, e.g., [1-8]. In particular, stable crack growth due to cyclic loading has been studied. This paper presents a stochastic model for this crack growth phase for which linear elastic fracture mechanics is applicable. A common model is formulated for constant and variable amplitude loading. The model is developed for a cracked panel and has been shown to be in good agreement with experimental test results. A generalization to a semi-elliptical

¹⁾ A.S VERITAS Research, P.O.Box 300, 1322 Hovik, Norway

²⁾ Polytechnic University, 333 Jay Street, Brooklyn, New York, 11201

³⁾ A.S VERITEC, P.O.Box 300, 1322 Hovik, Norway

surface crack is straightforward and has been successfully implemented. Uncertainties in the loading conditions, in the computation of the stress intensity factor, in the initial crack geometry, and in the material properties are included. In particular the material resistance against crack growth is modeled as a spatial random process thus accounting for material variations within each specimen.

The probability that the crack size exceeds a critical size during some time period is of interest. It is demonstrated how this event is formulated in terms of a limit state function with a corresponding safety margin and how the probability of failure can be calculated by a first- or second-order reliability method. The critical crack size may refer to growth through the thickness or to a size where a brittle fracture or plastic collapse occur. The critical crack size can be modeled as a deterministic or as a random quantity.

Inspections are frequently made for structures in service. Some inspections result in the detection of a crack while others give no detection. The size of a detected crack is measured either directly or indirectly through a non destructive inspection method, where the measured signal is interpreted as a crack size. Neither the measurement nor the interpretation are possible in an exact way and the resulting inspection result is consequently of random nature. When the inspection does not reveal a crack this does not necessarily mean that no crack is present. A detectable crack is only detected by a certain probability depending on the size of the crack and on the inspection method. Whether or not a crack is detected, the inspection provides additional information which can be used to update the reliability and/or the distribution of the basic variables. This can lead to, e.g., modifications of inspection plans, change in inspection method, or a decision on repair or replacement. The paper describes inspection results in terms of event margins and formulates the updating in terms of these event margins and the safety margin. The use of first-order reliability methods to perform the calculations is demonstrated.

When a repair of a detected crack is made and a new reliability analysis is performed, it is important that the new analysis accounts for the information that a repair was necessary. Often it is not possible to determine if the unexpected large crack size has been caused by a large initial size, by material properties poorer than anticipated, or by a loading of the crack tip area larger than anticipated. The paper demonstrates how information obtained in connection with a repair is introduced.

For welded structures a crack is generally assumed to be present after fabrication. The analysis method can, however, in a simple manner include a random crack initiation period for which a separate model can be formulated.

2. FATIGUE CRACK GROWTH MODEL

In a linear elastic fracture mechanics approach the increment in crack size, Δa , during a load cycle is related to the range of the stress intensity factor, ΔK , for the load cycle. A simple relation which is sufficient for most purposes was proposed by Paris and Erdogan, [9]

$$\Delta a = C (\Delta K)^m, \quad \Delta K > 0 \quad (1)$$

The crack growth equation is used without a positive lower threshold on ΔK below which no crack growth occurs. The equation was proposed based on experimental results, but is also the result of various mechanical and energy based models, see, e.g., [9,10]. C and m are material constants. The crack increment in one cycle is generally very small compared to the crack size and (1) is consequently written in a 'kinetic' form as

$$\frac{da}{dN} = C (\Delta K)^m, \quad \Delta K > 0 \quad (2)$$

where N is the number of stress cycles. The stress intensity factor K is computed by linear elastic fracture mechanics and is expressed as

$$K = \sigma Y(a) \sqrt{\pi a} \quad (3)$$

where σ is the far-field stress and $Y(a)$ is the geometry function. To explicitly account for uncertainties in the calculation of K , the geometry function is written as $Y(a) = Y(a, \mathbf{Y})$, where \mathbf{Y} is a vector of random parameters. Inserting (3) in (2) and separating the variables leads to the differential equation

$$\frac{da}{Y(a, \mathbf{Y})^m (\sqrt{\pi a})^m} = C \sigma^m dN, \quad a(0) = a_0 \quad (4)$$

where a_0 is the initial crack size. The equation is applied both for constant and for variable amplitude loading, thus ignoring possible sequence effects. Also a possible effect of the mean stress or R -ratio is ignored.

Eqs.(1-4) describe the crack size as a scalar a , which for a cracked panel is the crack length. For a surface or embedded crack a description of the crack depth, crack length and crack shape is necessary. It is common practice to assume a semi-elliptical or elliptical initial shape and to assume that the shape remains semi-elliptical or elliptical during the crack growth. In that case the crack depth a and the length $2c$ describe the crack. The differential equation (2) is replaced by a pair of coupled equations, see e.g. [11].

Solutions to (4) are smooth curves which do not intermingle. This is in contrast to experimental results as reported in, e.g., [12]. As a consequence the crack growth model is randomized as, [7]

$$\frac{da}{dN} = \frac{C_1}{C_2(a)} (\Delta K)^m \quad (5)$$

where C_1 is a random variable modeling variations in C from specimen to specimen, while $C_2(a)$ is a stationary log-normal process modeling variations in C within each specimen. The expected value of $C_2(a)$ is taken as one. The random model in (5) has three properties, which are experimentally observed in the test results reported in [12]:

- sample curves of a versus N are irregular and not very smooth,
- sample curves of a versus N become more smooth for larger values of a ,
- sample curves of a versus N intermingle, in particular for smaller values of a .

To estimate the correlation properties of the random process $C_2(a)$ a statistical analysis of the test data from [12] has been carried out, [7]. The correlation function $\rho_2(\Delta a)$ for $C_2(a)$ is shown to decrease to zero very rapidly with Δa . The correlation radius r_C is defined as

$$r_C = \int_{-\infty}^{\infty} \rho_2(x) dx \quad (6)$$

and has been estimated as 0.12 mm for the aluminum alloy in the experiments of [12]. The variance of C_2 has been estimated as 0.062 for the same data. The variance is expected to be significantly larger for crack growth in material in the heat affected zone or in the weld material. Non-proprietary data are, however, not available for estimation of the variance in these circumstances.

A damage function $\Psi(a)$ is introduced from (4) as

$$\Psi(a) = \int_{a_0}^a \frac{C_2(x)}{Y(x, \mathbf{Y})^m (\sqrt{\pi x})^m} dx \quad (7)$$

The stress ranges are denoted $S_i = \Delta\sigma_i$ and solution of (4) gives

$$\Psi(a) = C_1 \int_0^N S^m dN = \begin{cases} C_1 S^m N & \text{constant amplitude loading} \\ C_1 \sum_{r=1}^N S_r^m & \text{variable amplitude loading} \end{cases} \quad (8)$$

The difference between the two cases of constant and variable amplitude loading therefore only concerns the loading statistics. In the remaining part of the paper constant amplitude loading is considered.

In the presentation it has so far been assumed that a crack is present at the time the loading is applied. With an initial crack initiation period before the crack reaches a size a_0 for which fracture mechanics can be applied to describe the fatigue crack growth with some confidence, the solution to (4) is

$$\int_{a_0}^a \frac{C_2(x)}{Y(x, Y)^m (\sqrt{\pi x})^m} dx = C_1 S^m (N - N_0) \quad (9)$$

where N_0 is the (random) crack initiation period for which a separate model can be formulated.

The second moment statistics for the damage function conditioned upon (a_0, Y, m) are

$$E[\Psi(a) | a_0, Y, m] = \int_{a_0}^a \frac{E[C_2(x)]}{Y(x, Y)^m (\sqrt{\pi x})^m} dx = \int_{a_0}^a \frac{1}{Y(x, Y)^m (\sqrt{\pi x})^m} dx \quad (10)$$

$$Var[\Psi(a) | a_0, Y, m] = \int_{a_0}^a \int_{a_0}^a \frac{Cov[C_2(x_1), C_2(x_2)]}{Y(x_1, Y)^m (\sqrt{\pi x_1})^m Y(x_2, Y)^m (\sqrt{\pi x_2})^m} dx_1 dx_2 \quad (11)$$

$$\approx r_{C_2} Var[C_2] \int_{a_0}^a \frac{1}{Y(x, Y)^{2m} (\pi x)^m} dx$$

$$\rho[\Psi(a_1), \Psi(a_2) | a_0, Y, m] \approx \frac{\int_{a_0}^{\min(a_1, a_2)} \frac{1}{Y(x, Y)^{2m} (\pi x)^m} dx}{\left(\int_{a_0}^{a_1} \frac{dx_1}{Y(x_1, Y)^{2m} (\pi x_1)^m} \right)^{1/2} \left(\int_{a_0}^{a_2} \frac{dx_2}{Y(x_2, Y)^{2m} (\pi x_2)^m} \right)^{1/2}} \quad (12)$$

The approximations for the variance and the correlation function are justified by the short correlation length of $C_2(a)$ compared to crack size increments of interest. The random variable $\Psi(a) | a_0, Y, m$ is essentially the sum of many independent random variables of approximately the same variance. The distribution is therefore well approximated by a normal distribution.

The failure criterion is taken as exceedence of a critical crack size a_c in a time period with N stress cycles,

$$a_c - a_N \leq 0 \quad (13)$$

where a_N is the crack size after the N stress cycles. $\Psi(a)$ is monotonically increasing and the failure criterion (13) can be written as

$$\Psi(a_c) - \Psi(a_N) = \int_{a_0}^{a_c} \frac{C_2(x)}{Y(x, Y)^m (\sqrt{\pi x})^m} dx - C_1 S^m N \leq 0 \quad (14)$$

The safety margin M is therefore defined as

$$M = \int_{a_0}^{a_c} \frac{C_2(x)}{Y(x, Y)^m (\sqrt{\pi x})^m} dx - C_1 S^m N \quad (15)$$

and the failure probability P_F is

$$P_F = P(M \leq 0) \quad (16)$$

3. EVENT MARGINS FOR INSPECTION RESULTS AND REPAIR

Two types of inspection results are considered

$$a(N_i) \leq A_{di}, \quad i=1,2,\dots,r \quad (17)$$

$$a(N_j) = A_j, \quad j=1,2,\dots,s \quad (18)$$

In the first case, (17), no crack was found in the inspection after N_i stress cycles, implying that the crack size was smaller than the smallest detectable crack size A_{di} . A_{di} is generally random since a detectable crack is only detected with a certain probability depending on the crack size and on the inspection method. The distribution of A_{di} is the distribution of non-detected cracks. Information of the type (17) can be envisaged for several times. If A_{di} is deterministic, however, and the same for all inspections, the information in the latest observation contains all the information of the previous ones. In the second case, (18), a crack size A_j is observed after N_j stress cycles. A_j is generally random due to measurement error and/or due to uncertainties in the interpretation of a measured signal as a crack size. Measurements of the type (18) can also be envisaged for several times corresponding to several values of N_j .

For each measurement (17) an event margin M_i can be defined similar to the safety margin (15) as

$$M_i = C_1 S^m N_i - \int_{a_0}^{A_{di}} \frac{C_2(x)}{Y(x, Y)^m (\sqrt{\pi x})^m} dx \leq 0, \quad i=1,2,\dots,r \quad (19)$$

These event margins are negative due to (17). For each measurement (18) an event margin can similarly be defined as

$$M_j = \int_{a_0}^{A_j} \frac{C_2(x)}{Y(x, Y)^m (\sqrt{\pi x})^m} dx - C_1 S^m N_j = 0, \quad j=1,2,\dots,s \quad (20)$$

These safety margins are zero due to (18).

The situation is envisaged where no crack is detected in the first r inspections at a location, while a crack is detected by the $r+1$ 'th inspection and its size is measured at this and the following $s-1$ inspections. The updated failure probability is in this case

$$P_F = P(M \leq 0 | M_1 \leq 0 \cap \dots \cap M_r \leq 0 \cap M_{r+1} = \dots = M_{r+s} = 0) \quad (21)$$

A more general situation involves simultaneous consideration of several locations with potentially dangerous cracks for which inspections are carried out. The updating procedure still applies when due consideration is taken to the dependence between basic variables referring to different locations.

Assuming that a repair takes place after N_{rep} stress cycles and a crack size a_{rep} is observed. The event margin M_{rep} is defined as

$$M_{rep} = \int_{a_0}^{a_{rep}} \frac{C_2(x)}{Y(x, Y)^m (\sqrt{\pi x})^m} dx - C_1 S^m N_{rep} = 0 \quad (22)$$

The crack size present after repair and a possible inspection is a random variable a_{new} and the material properties after repair are m_{new} and $C_{1,new}$. The safety margin after repair is M_{new}

$$M_{new} = \int_{a_{new}}^{a_c} \frac{C_2(x)}{Y(x, Y)^{m_{new}} (\sqrt{\pi x})^{m_{new}}} dx - C_{1,new} S^{m_{new}} (N - N_{rep}) \quad (23)$$

and the failure probability after repair is

$$P_F = P(M_{new} \leq 0 | M_{rep} = 0) \quad (24)$$

This updated failure probability is then of the same form as (21).

4. RELIABILITY METHOD

The reliability method used in this paper is the first-order reliability method which is here briefly reviewed for parallel systems. For a more thorough description see [13]. Each element in the parallel system is described by a safety margin $M_i = g_i(Z)$ in terms of the vector of basic variables Z . The safety margins are defined with $M_i \leq 0$ corresponding to failure in the i th element, and $g_i(z) = 0$ defining the limit state surface for the i th element. The failure probability of a parallel system with k elements is

$$P_F = P(M_1 \leq 0 \cap M_2 \leq 0 \cap \dots \cap M_k \leq 0) \quad (25)$$

The failure probability is computed efficiently and to a good accuracy by a first-order reliability method. The first step in the computation is a transformation of the vector of basic variables into a vector of standardized and independent normal variables U . The transformation is denoted T and the transformed space is called the normal space.

$$U = T(Z) \quad (26)$$

A good choice for T is a transformation, which uses the conditional distribution functions $F_i(z_i | z_1, \dots, z_{i-1}) = P(Z_i \leq z_i | Z_1 = z_1, \dots, Z_{i-1} = z_{i-1})$ of the basic variables, [14]

$$\begin{aligned} U_1 &= \Phi^{-1}(F_1(Z_1)) \\ U_2 &= \Phi^{-1}(F_2(Z_2 | Z_1)) \\ &\vdots \\ U_i &= \Phi^{-1}(F_i(Z_i | Z_1, Z_2, \dots, Z_{i-1})) \\ &\vdots \\ U_n &= \Phi^{-1}(F_n(Z_n | Z_1, Z_2, \dots, Z_{n-1})) \end{aligned} \quad (27)$$

Here $\Phi(\cdot)$ denotes the standardized normal distribution function. The limit state surfaces for the individual elements are expressed in terms of u as

$$g_i(z) = g_i(T^{-1}(u)) = g_{u,i}(u) = 0, \quad i = 1, 2, \dots, k \quad (28)$$

The second step in a first-order reliability analysis consists in determining the joint design point u^* , which is the point on the limit state surface closest to the origin. u^* is thus found as the solution of a constrained minimization

$$\begin{aligned} \min |u| \\ g_{u,i}(u) \leq 0, \quad i = 1, 2, \dots, k \end{aligned} \quad (29)$$

provided that $g_{u,i}(0) > 0$ for at least one $i \in \{1, \dots, k\}$. Standard optimization techniques can be applied to solve this problem. All constraints are not necessarily active at the joint design point, i.e., $g_{u,i}(u) = 0$ is not necessarily valid for all i . Let $l \leq k$ denote the number of active constraints.

The third step in a first-order reliability method consists in a linearization of the safety margins at the joint design point formulated in the normal space. In normalized form the linearized safety margins are

$$M_i = \beta_i - \alpha_i^T U \quad (30)$$

where α_i is a unit vector and β_i is the first-order reliability index for element i of the parallel system linearized at the joint design point. The correlation coefficient ρ_{ij} between the safety margins M_i and M_j is

$$\rho_{ij} = \rho[M_i, M_j] = \alpha_i^T \alpha_j \quad (31)$$

The failure probability of the parallel system is now estimated as

$$P_F \approx \Phi_l(-\beta; \rho) \quad (32)$$

where $\beta = \{\beta_i\}$, $\rho = \{\rho_{ij}\}$ and only the l active elements are included. The asymptotic result as $|u^*| \rightarrow \infty$ is, [15]

$$P_F \sim \Phi_l(-\beta; \rho) [\det(I-D)]^{-1/2}, \quad |u^*| \rightarrow \infty \quad (33)$$

where I denotes the unit matrix and D is a matrix determined by the coordinates of the design point and the gradients and second order derivatives of the limit state functions at the design point.

The reliability index β_R for the system is defined as

$$\beta_R = -\Phi^{-1}(P_F) \quad (34)$$

For a single element the asymptotic result for β_R is derived in [16]:

$$\beta_R \sim \beta, \quad \beta = |u^*| \rightarrow \infty \quad (35)$$

A generalization of this result to a parallel system yields

$$\beta_R \sim -\Phi^{-1}(\Phi_l(-\beta; \rho)), \quad |u^*| \rightarrow \infty \quad (36)$$

The failure probability in (16) is calculated directly by (32) or (33) with $k=l=1$. The updated failure probability in (21) is rewritten as

$$\begin{aligned} & P(M \leq 0 | M_1 \leq 0 \cap \dots \cap M_r \leq 0 \cap M_{r+1} = \dots = M_{r+s} = 0) \quad (37) \\ &= \frac{\partial^s P(M \leq 0 \cap M_1 \leq 0 \cap \dots \cap M_r \leq 0 \cap M_{r+1} \leq x_{r+1} \cap \dots \cap M_{r+s} \leq x_{r+s})}{\partial x_{r+1} \dots \partial x_{r+s}} \\ &= \frac{\partial^s P(M_1 \leq 0 \cap \dots \cap M_r \leq 0 \cap M_{r+1} \leq x_{r+1} \cap \dots \cap M_{r+s} \leq x_{r+s})}{\partial x_{r+1} \dots \partial x_{r+s}} \end{aligned}$$

where the partial derivatives are evaluated at $x=0$. Two parallel systems must thus be analyzed, but the optimization problem is cast in a slightly different form than (29) since the constraints corresponding to the detected crack sizes are changed to equality constraints. In addition, linearized safety margins for inactive constraints are included as described in [17]. The vector of reliability indices and the correlation matrix for the normalized safety and event margins in the numerator are

$$\begin{bmatrix} \beta \\ \beta_1 \\ \beta_2 \end{bmatrix}, \quad \begin{bmatrix} 1 & \rho_1^T & \rho_2^T \\ \rho_1 & \rho_{11} & \rho_{21}^T \\ \rho_2 & \rho_{21} & \rho_{22} \end{bmatrix} \quad (38)$$

where β refer to the safety margin, an index 1 to the normalized event margins for no detection and an index 2 to the normalized event margins for a detected crack and measured crack size. The dimension of β_1 is r (since inactive constraints have been included) and the dimension of β_2 is s . The vector of reliability indices and the correlation matrix for the denominator are similarly

$$\begin{bmatrix} \beta_1' \\ \beta_2' \end{bmatrix}, \quad \begin{bmatrix} \rho_{11}' & \rho_{21}'^T \\ \rho_{21}' & \rho_{22}' \end{bmatrix} \quad (39)$$

The joint design point for the parallel system in the denominator is generally different from the design point of the parallel system in the numerator which is emphasized by the prime. The dimension of β_1' is r and the dimension of β_2' is s .

In [18] the asymptotic result for the partial derivative of β_R for an element has been derived with respect to a distribution or limit state function parameter p :

$$\frac{\partial \beta_R}{\partial p} \sim \frac{\partial \beta}{\partial p}, \quad |u^*| \rightarrow \infty \quad (40)$$

For the failure probability then follows

$$\frac{\partial P_F}{\partial p} = \frac{\partial \Phi(-\beta_R)}{\partial p} = -\phi(\beta_R) \frac{\partial \beta_R}{\partial p} \sim -\phi(\beta) \frac{\partial \beta}{\partial p}, \quad |u^*| \rightarrow \infty \quad (41)$$

Generalizing this result to the parallel system in the numerator of (37) yields

$$\frac{\partial^s P(M \leq 0 \cap M_1 \leq 0 \cap \dots \cap M_r \leq 0 \cap M_{r+1} \leq x_{r+1} \cap \dots \cap M_{r+s} \leq x_{r+s})}{\partial x_{r+1} \dots \partial x_{r+s}} \Big|_{x=0} \quad (42)$$

$$\sim \frac{\partial^s \Phi_{r+s+1} \left[- \begin{bmatrix} \beta \\ \beta_1 \\ \beta_2 \end{bmatrix}; \begin{bmatrix} 1 & \rho_1^T & \rho_2^T \\ \rho_1 & \rho_{11} & \rho_{21}^T \\ \rho_2 & \rho_{21} & \rho_{22} \end{bmatrix} \right]}{\partial \beta_{r+1} \dots \partial \beta_{r+s}} \\ = \phi_s(-\beta_2; \rho_{22}) \Phi_{r+1} \left[- \left[\begin{bmatrix} \beta \\ \beta_1 \end{bmatrix} - \begin{bmatrix} \rho_2^T \\ \rho_{21}^T \end{bmatrix} \rho_{22}^{-1} \beta_2 \right]; \left[\begin{bmatrix} 1 & \rho_1^T \\ \rho_1 & \rho_{11} \end{bmatrix} - \begin{bmatrix} \rho_2^T \\ \rho_{21}^T \end{bmatrix} \rho_{22}^{-1} [\rho_2 \ \rho_{21}] \right] \right]$$

where standard results for the conditional multivariate normal distribution have been applied since the vectors of linearized safety margins are joint normally distributed. Furthermore $\partial \beta_i / \partial x_i = -1$ has been used, which is valid since $Var[M_i] = 1$. For the conditional probability in (37) one obtains:

$$P(M \leq 0 | M_1 \leq 0 \cap \dots \cap M_r \leq 0 \cap M_{r+1} = \dots = M_{r+s} = 0) \quad (43)$$

$$\sim \frac{\phi_s(-\beta_2; \rho_{22})}{\phi_s(-\beta_2'; \rho_{22}')} \frac{\Phi_{r+1} \left[- \left[\begin{array}{c} \beta \\ \beta_1 \end{array} \right] - \left[\begin{array}{c} \rho_2^T \\ \rho_{21}^T \end{array} \right] \rho_{22}^{-1} \beta_2; \left[\begin{array}{cc} 1 & \rho_1^T \\ \rho_1 & \rho_{11} \end{array} \right] - \left[\begin{array}{c} \rho_2^T \\ \rho_{21}^T \end{array} \right] \rho_{22}^{-1} [\rho_2 \ \rho_{21}] \right]}{\Phi_r(-\beta_1' + \rho_{21}^T(\rho_{22}')^{-1}\beta_2'; \rho_{11}' - \rho_{21}^T(\rho_{22}')^{-1}\rho_{21}')}$$

The updating of the reliability has been demonstrated. If the interest is on updating the distribution of the basic variables the same procedure is followed. Instead of the safety margin (15) an event margin M for basic variable Z_i is defined as

$$M = Z_i - z_i \quad (44)$$

With the safety margin replaced by this event margin the value of the cumulative distribution function for Z_i at the argument z_i is updated. The procedure can be repeated for different arguments z_i and the complete distribution function thereby be updated. Even when the basic variables are initially independent the updating procedure generally introduces dependence. It may thus be more relevant to update the joint distribution function. The safety margin M is then replaced by a vector of event margins $\{Z_i - z_i\}, i = 1, \dots, n$ and the updating of the vector is performed as described above. In connection with a reanalysis after repair it is important that the updated distributions are used.

5. EXAMPLE.

Consider a panel with a center crack as in the experiments of [12]. The loading is a constant amplitude loading leading to a far-field stress range S . The geometry function is modeled as

$$Y(a, Y) = \exp(Y_1 (\frac{a}{50})^{Y_2}) \quad (45)$$

The geometry function takes the value one for $a = 0$. Lengths are measured in mm and stresses in N/mm^2 . The distribution of the basic variables is taken as

$$\left\{ \begin{array}{l} S \in N(60, 10^2) \\ Y_1 \in LN(1, 0.2^2) \\ Y_2 \in LN(2, 0.1^2) \\ a_0 \in EX(1) \\ a_c \in N(50, 10^2) \\ (\ln C_1, m) \in N_2(-33.00, 0.47^2, 3.5, 0.3^2; -0.9) \end{array} \right. \quad (46)$$

$N(\mu, \sigma^2)$ denotes a normal distribution with mean value μ and variance σ^2 . Similarly $LN(\mu, \sigma^2)$ denotes a log-normal distribution with mean value μ and variance σ^2 . $N_2(\mu_1, \sigma_1^2, \mu_2, \sigma_2^2; \rho)$ denotes a bivariate normal distribution with mean values μ_1 and μ_2 , variances σ_1^2 and σ_2^2 and correlation coefficient ρ . $EX(\mu)$ denotes an exponential distribution with mean value μ . The negative correlation between $\ln C_1$ and m is not reflecting a physical dependence, but is introduced by the form of the crack growth equation (2). Statistics for $C_2(a)$ are taken as those reported in [7], see section 2 of this paper. The example has eight basic variables and the transformation into standardized and independent normal variables has been described in [13,19,20].

The first-order and improved second-order approximations to the reliability index are shown in Fig.1 for various life times expressed in terms of the number of stress cycles N . The two approximations are close implying that the curvatures of the limit state surface are moderate at the design point.

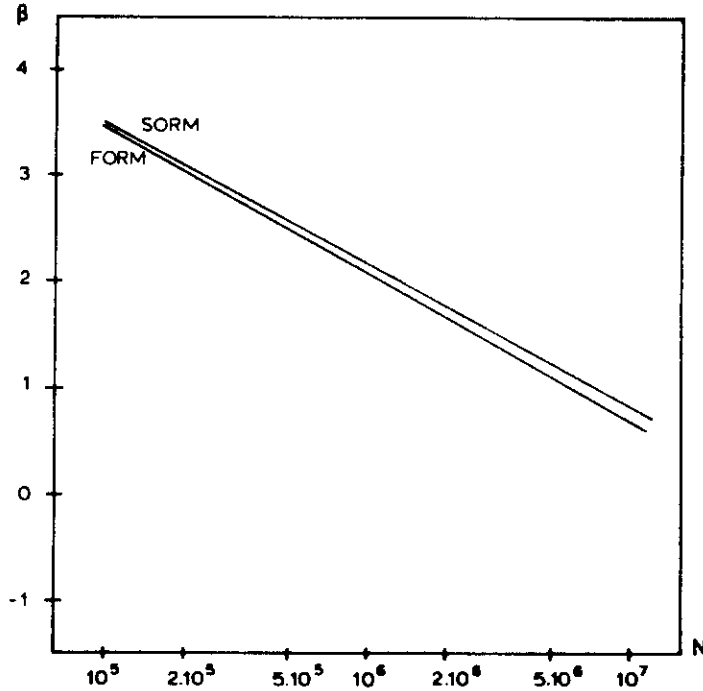


Figure 1. First- and second-order reliability index from design calculation. Statistics for the distribution of life time T can be directly approximated from the results of Fig.1. For the mean life times the approximation is

$$E[T] = \int_0^{\infty} (1 - P(T \leq t)) dt \approx \int_0^{\infty} \Phi(\beta(t)) dt \quad (47)$$

For $N=1.5 \cdot 10^6$ cycles the reliability index and the sensitivity factors are shown in Table 1. α_i^2 can be interpreted as the fraction of the total uncertainty due to uncertainty arising from basic variable U_i . The major contribution to the overall uncertainty is thus in this case from the uncertainty in the material parameters. The critical crack size uncertainty is of little relative importance in this case, and the same is concluded in almost all cases where the critical crack size is significantly larger than the initial crack size. The uncertainty in the geometry function contributes very little to the total uncertainty in this case. This is because the value for $a=0$ is completely known. When this initial value is not known the uncertainty is comparable to the uncertainty in the loading. The uncertainty contribution from the uncertainty in the change in the geometry function from the initial value is generally found to be low. For tubular joints, where the geometry function is approximately proportional to $a^{-1/2}$ for large values of a , this statement may not be true in all cases.

Based on the results in Table 1 and results for the parametric sensitivity factor (40), [13,18], the sensitivity of the reliability index to a change in a distribution parameter can be determined. For the mean value μ_S of the normally distributed loading variable S , the sensitivity factor is

$$\frac{\partial \beta}{\partial \mu_S} = -\frac{\alpha_S}{\sigma_S} = -\frac{0.358}{10} = -0.0358 \quad (48)$$

TABLE 1 Reliability index and sensitivity factors

Variable	$\beta=1.816$	
	$N=1.5 \cdot 10^6$	α_i^2
a_0	0.5513	30%
a_C	-0.0001	0%
S	0.3577	13%
m	-0.6141	38%
$C m$	0.4362	19%
Y_1	-0.0248	0%
Y_2	0.0085	0%
$\Psi(a_C) a_0, a_C, Y, m$	-0.0060	0%

An increase in μ_S by 10 MPa thus leads to an change in β of approximately $(-0.0358)10=-0.358$.

Next, the situation where a crack is found in the first inspection is considered. It is envisaged that the inspection is carried out after $N_1=10^5$ stress cycles and a crack length of 3.9 mm is measured. The measurement error is assumed to be normally distributed with standard deviation σ_A . Figure 2 shows the updated reliability index as a function of σ_A , when (43) has been applied with $(r, s)=(0, 1)$. The result is almost independent of σ_A in this example as the uncertainty in the initial crack size is dominating the uncertainty in A_1 .

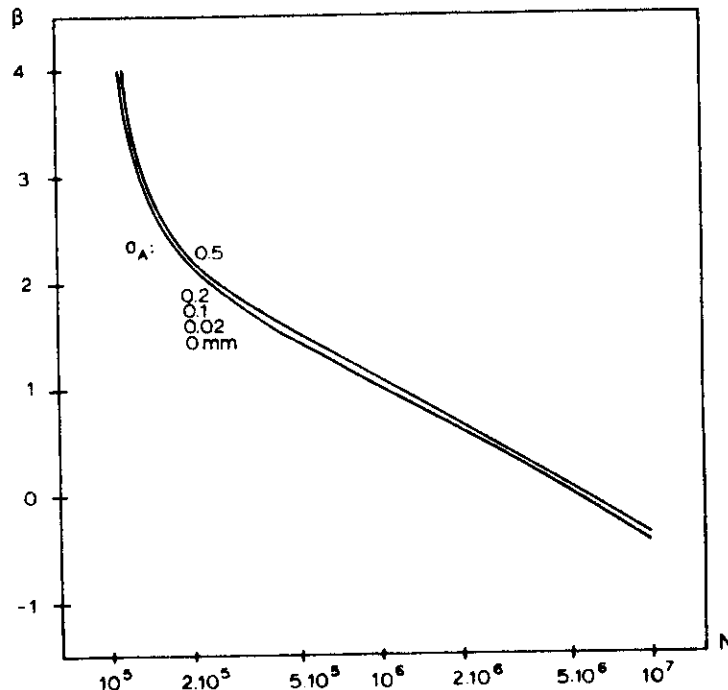


Figure 2. Updated first-order reliability index after first inspection with crack measurement 3.9 mm.

When the crack is detected, a decision has to be made and two options are present. It may be decided to repair the crack now or to leave the crack as it is and base a decision on repair on more inspection results. With just one inspection it is not possible to determine if the crack was initially large but grows slowly enough that repair is not needed, or the crack was initially fairly small but is growing fast and must be repaired. If a requirement

on the reliability index in a period without inspections is formulated, e.g., $\beta_R \geq 2$, the latest time of the next inspection is determined from Fig.2.

Assume that the crack is not repaired but a second inspection at $N=2 \cdot 10^5$ stress cycles is required. Let the inspection method be the same as in the first inspection and let the measured crack size be 4.0 mm. The measurement error is again assumed to be normally distributed with standard deviation σ_A and the two measurement errors are assumed to be statistically independent. Figure 3 shows the updated reliability index after this second inspection.

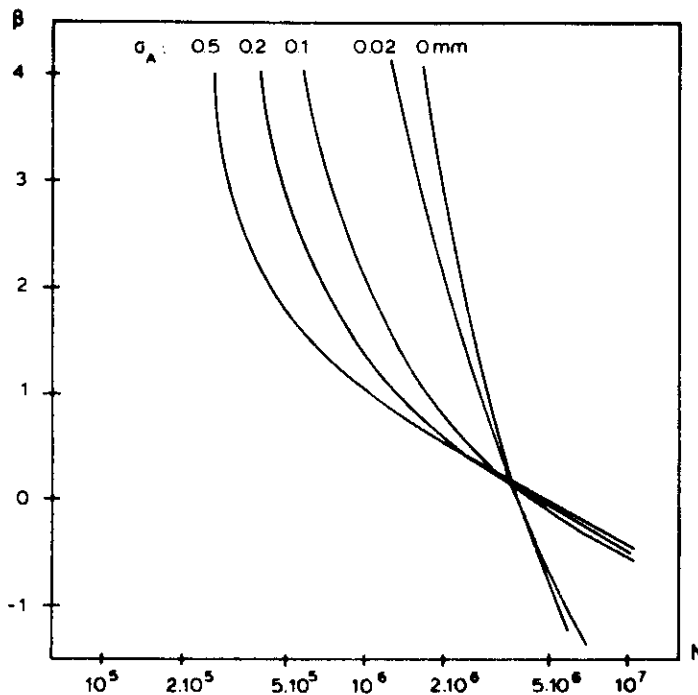


Figure 3. Updated first-order reliability index after second inspection with crack measurements 3.9 mm and 4.0 mm.

Different inspection qualities now lead to very different results. With $\sigma_A = 0$ the negative slope of the reliability index curve becomes very large demonstrating that the crack growth behavior is basically determined by two combinations of the basic variables. With a large measurement uncertainty there is an immediate and large increase in reliability, but after some time the curve becomes almost identical to the curve resulting after the first inspection. Due to large uncertainty in both inspections only little information is gained on the crack growth rate. If the inspection quality is very high it may be possible to state that the crack does not grow to a critical size within the design life time. Repair and further inspections are then unnecessary. For a poorer inspection quality a time period until the next inspection can be determined and the decision on repair be further delayed.

Figure 4 shows the results of Fig.3 together with similar results for a homogeneous material. It is observed that only for very small inspection uncertainty does the material inhomogeneity significantly affect results. The estimates for material inhomogeneity used in this example are for base material and the conclusion may be somewhat different for crack growth in weld material or in material in a heat affected zone.

Figure 5 presents results similar to those in Fig.3, but for the case where a crack size of 5 mm is reported in the second inspection. Together, the two inspection results now indicate that a large and fast growing crack is present. Repair is therefore necessary within a short period.

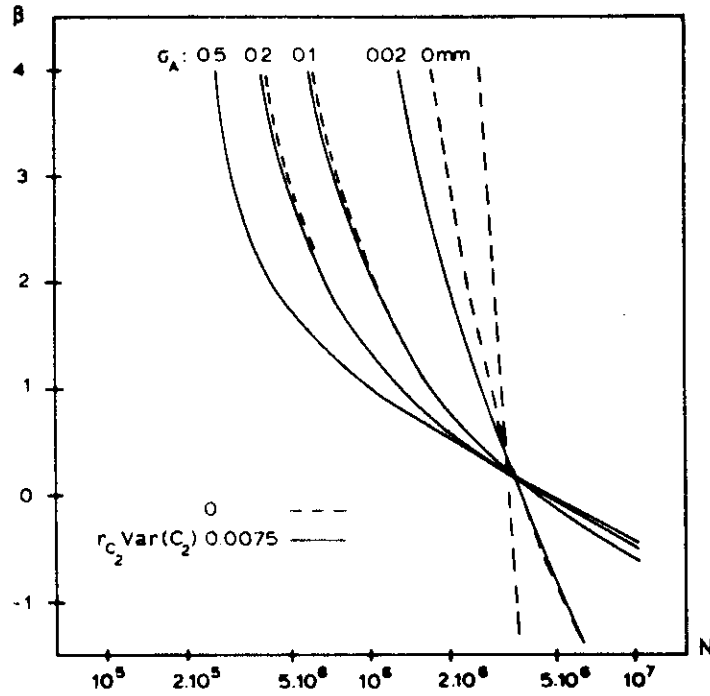


Figure 4. Updated first-order reliability index after second inspection with crack measurements 3.9 mm and 4.0 mm, importance of inhomogeneity.

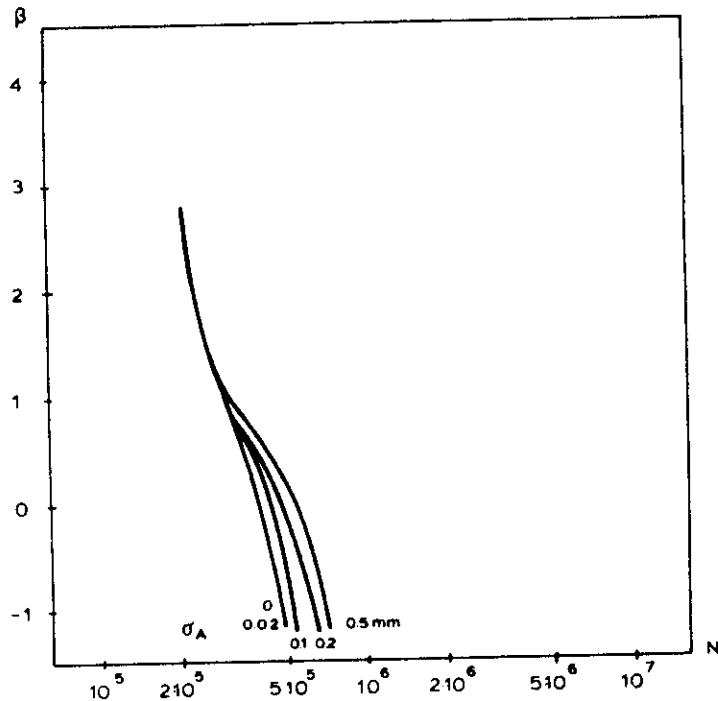


Figure 5. Updated first-order reliability index after second inspection with crack measurements 3.9 mm and 5.0 mm.

Consider now different situations where the inspections do not result in crack detection. An attempt is made to illustrate possible means to achieve a required reliability. Let the reliability requirement be $\beta_R \geq 3.0$ and let the design life time correspond to $1.5 \cdot 10^6$ stress cycles.

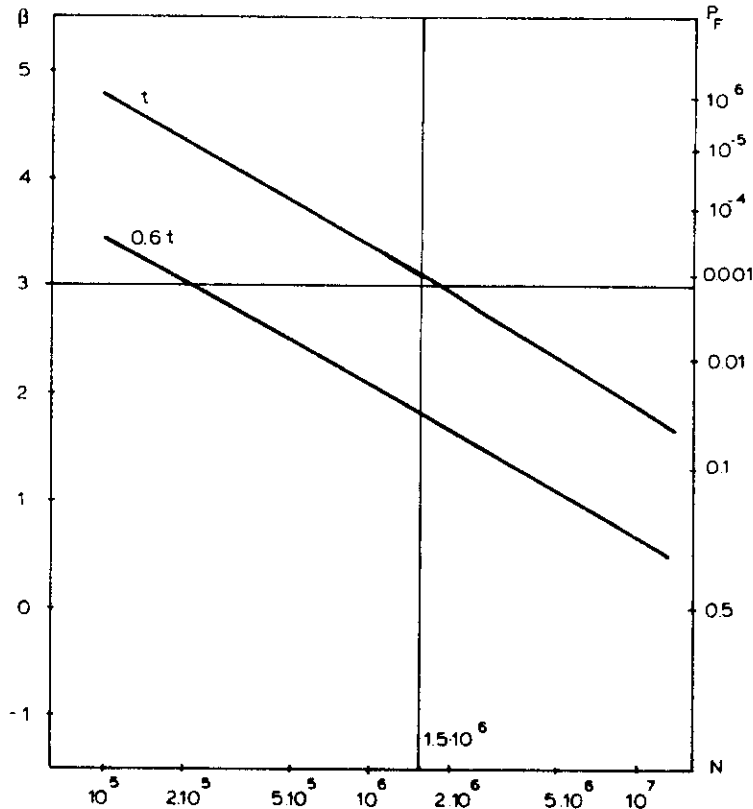


Figure 6. First-order reliability index for two plate thicknesses.

Figure 6 shows the reliability index as a function of number of stress cycles for two plate thicknesses. With a plate thickness t the reliability requirement is fulfilled for the design life time and no inspections are needed. With a plate thickness of only 60% of t the reliability requirement is fulfilled for the period until $N=2 \cdot 10^5$ stress cycles, where an inspection is needed. The quality of the inspection is reflected in the distribution of non-detected cracks. An exponential distribution is assumed with a mean value λ . Cracks initially present are cracks which have passed the inspection at the production site either because they were not detected or because they were below the acceptance level. If no cracks were accepted in fabrication, the fabrication inspection therefore corresponds to $\lambda=1$.

Figure 7 shows the initial reliability index and updated reliability indices for three inspection qualities. The best inspection quality $\lambda=0.3$ is better than the fabrication inspection quality and if no crack is found with this method the increase in reliability is sufficient to make further inspections unnecessary. For the two other inspection qualities, periods are determined until the next inspection.

Figure 8 shows the total inspection requirement for $\lambda=1$ when no crack is detected in any inspection. For this case two inspections are needed. Finally, Fig.9 shows the total inspection requirement for $\lambda=3$ when no crack is detected in any inspection, and for this case five inspections are needed. It is thus demonstrated that different strategies on design and inspection planning can be used to achieve a required reliability. Based on costs of each strategy including expected failure costs a cost optimal solution can be determined.

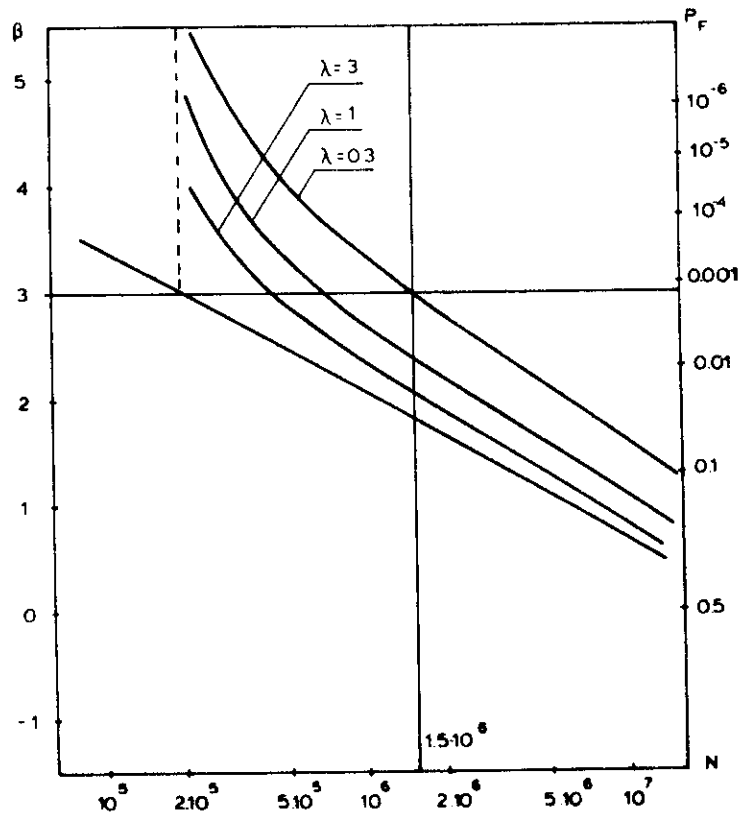


Figure 7. Updated first-order reliability index after first inspection with no crack detection.

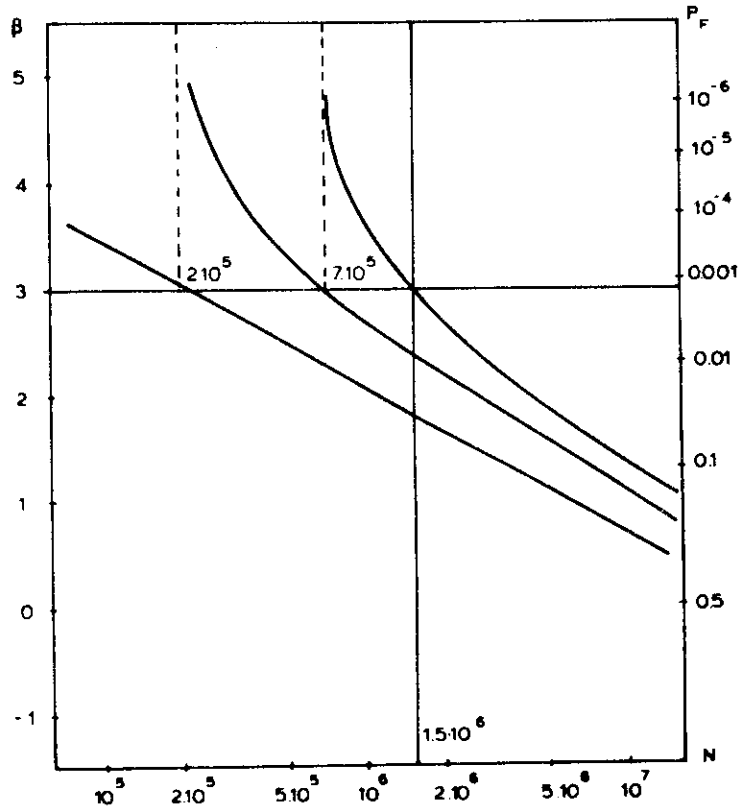


Figure 8. Updated first-order reliability index after inspections with no crack detection, mean size of non-detected cracks 1 mm.

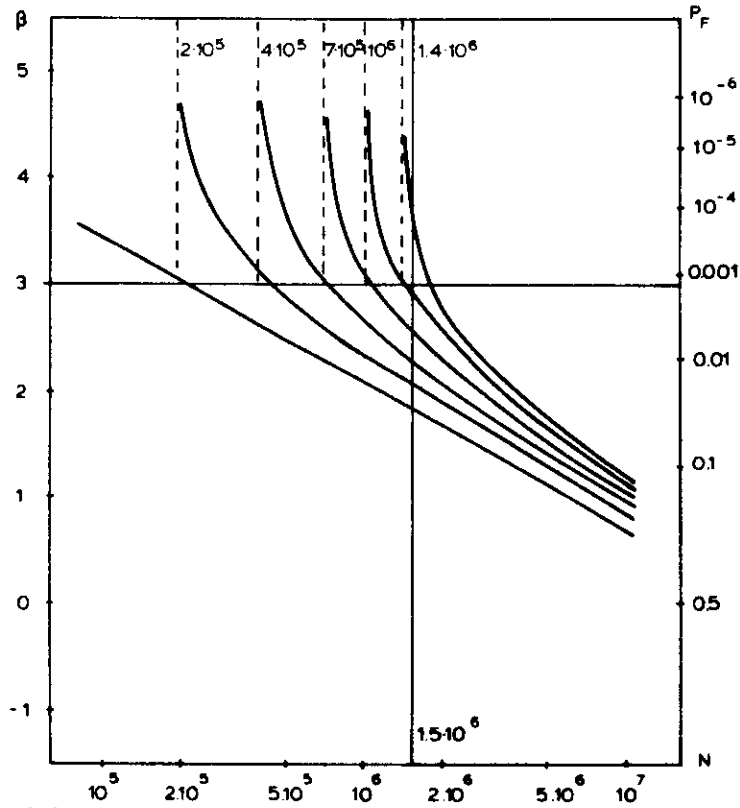


Figure 9. Updated first-order reliability index after inspections with no crack detection, mean size of non-detected cracks 3 mm.

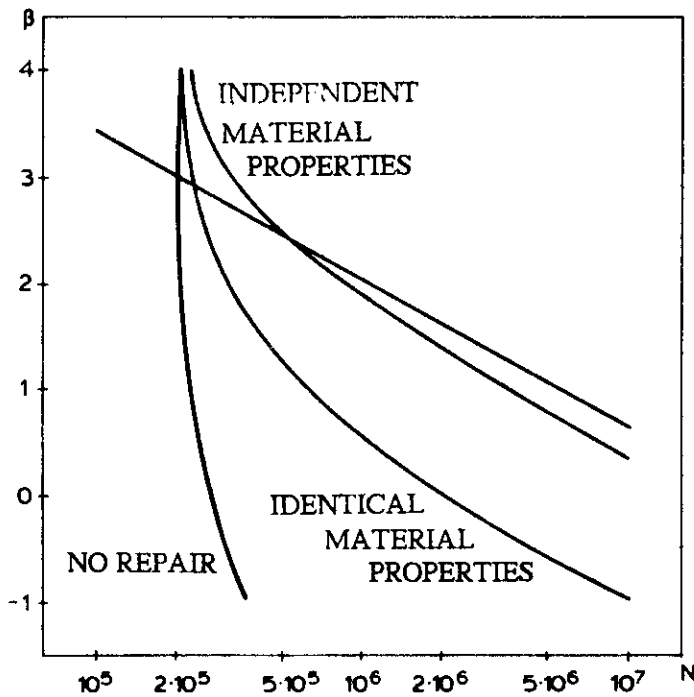


Figure 10. Updated first-order reliability index after repair of an 8 mm crack at $N = 2 \cdot 10^5$ stress cycles.

The results of a reliability analysis following a repair of a detected crack is illustrated in Fig.10. It is assumed that a crack size of $a_{rep} = 8$ mm is repaired after $N_{rep} = 2 \cdot 10^5$ stress cycles. The distribution of the initial crack size after repair a_{new} is taken as an exponential distribution with a mean value of 1 mm, i.e., as the same initial distribution as after fabrication. Two situations are considered with either identical or independent material properties before and after repair. When independent properties are assumed the same distribution is used for the properties before and after repair. It follows from the results that there is an immediate increase in reliability after repair, but the reliability quickly drops to a level below the level obtained for the calculations before repair. This reflects the possibility that the cause for the large repaired crack size is a larger than anticipated loading of the crack tip, which is also acting after the repair.

The results presented in this example have been for a constant amplitude loading. For offshore structures a long term stress range distribution is generally applied in fatigue analyses. Due to uncertainty in the environmental statistics, load models, global structural analysis and local stress analysis, the parameters of the long term distribution should be modeled as random variables. A Weibull distribution is often used

$$F_S(s) = 1 - \exp(-(s/A)^B), \quad s > 0 \quad (49)$$

where A and B are random variables. A calibration of the statistics for A and B , based on an uncertainty modeling for the above mentioned sources, can be performed by a modification of the probabilistic fatigue analysis presented in [21]. The factor $\sum_{r=1}^N S_r^m$ in (8) is replaced by the expected value, which for Weibull distributed stress ranges becomes

$$E\left[\sum_{r=1}^N S_r^m\right] = E[N]E[S^m] = E[N]A^m \Gamma\left(1 + \frac{m}{B}\right) \quad (50)$$

The expected value is random due to the random distribution parameters, but the uncertainty in the sum for fixed distribution parameters is neglected. This is reasonable due to the large number of random variables with little correlation in the summation.

6. CONCLUSIONS

The following conclusions can be stated:

- 1) A stochastic model for fatigue crack growth has been applied which accounts for uncertainties in loading, initial defects, critical crack size, material parameters including spatial variation, and in the computation of the stress intensity factor. Based on the crack growth model and a load model a safety margin has been defined.
- 2) Two types of inspection results have been considered and the inspection uncertainty has been modeled. Event margins have been defined for both types of inspection results. Updated reliabilities have been expressed in terms of the safety margin and the inspection event margins. A similar analysis has been performed for a structure after repair.
- 3) A brief discussion of first-order reliability theory applied to parallel systems has been presented. It has been demonstrated that the updating after inspection and repair can be carried out in a simple way by use of first-order reliability methods. Updating of the reliability and/or of the distribution of the basic variables have been considered.
- 4) The analysis has been presented for an example panel with a center crack. The reliability index has been computed based on information at the design stage and has been updated based on inspection results both resulting in crack detection and in no detection. The effect of material inhomogeneity for the selected base material has been

demonstrated to be insignificant. Different inspection qualities have been considered resulting in different effects on the updated reliability index.

7. REFERENCES

- [1] Kozin, F. and J. L. Bogdanoff, 'A Critical Analysis of Some Probabilistic Models for Fatigue Crack Growth,' *Engineering Fracture Mechanics*, Vol. 14, 1981, pp. 59-89.
- [2] Arone, R., 'On Reliability Assessment for a Structure with a System of Cracks,' in *DIALOG 6-82*, Danish Engineering Academy, Lyngby, Denmark, 1983.
- [3] Series of Articles by the ASCE Committee on Fatigue and Fracture Reliability, *Journal of the Structural Division*, ASCE, Vol. 108, 1982, pp. 3-88.
- [4] Lin, Y. K. and J. N. Yang, 'On Statistical Moments of Fatigue Crack Propagation,' *Engineering Fracture Mechanics*, Vol. 18, 1983, pp. 243-256.
- [5] Madsen, H. O., 'Probabilistic and Deterministic Models for Predicting Damage Accumulation due to Time Varying Loading,' *DIALOG 5-82*, Danish Engineering Academy, Lyngby, Denmark, 1983.
- [6] Bolotin, V. V., *Wahrscheinlichkeitsmethoden zur Berechnung von Konstruktionen*, VEB Verlag für Bauwesen, Berlin, 1981.
- [7] Ortiz, K. and A. S. Kiremidjian, 'Time Series Analysis of Fatigue Crack Growth Data,' submitted to *Engineering Fracture Mechanics*, 1985.
- [8] Ditlevsen, O., 'Random Fatigue Crack Growth - A First Passage Problem,' *Engineering Fracture Mechanics*, Vol. 23, 1986, pp. 467-477.
- [9] Paris, P. and F. Erdogan, 'A Critical Analysis of Crack Propagation Laws,' *Journal of Basic Engineering*, Trans. ASME, Vol. 85, 1963, pp. 528-534.
- [10] Irving, P. E. and L. N. McCartney, 'Prediction of Fatigue Crack Growth Rates: Theory, Mechanisms and Experimental Results,' Fatigue 77 Conference, University of Cambridge, in *Metal Science*, Aug./Sept. 1977, pp. 351-361.
- [11] Shang-Xian, W., 'Shape Change of Surface Crack During Fatigue Growth,' *Engineering Fracture Mechanics*, Vol. 22, 1985, pp. 897-913.
- [12] Virkler, D. A., Hilberry, B. M. and P. K. Goel, 'The Statistical Nature of Fatigue Crack Propagation,' *Journal of Materials and Technology*, Vol. 101, 1979, pp. 148-153.
- [13] Madsen, H. O., Krenk, S. and N. C. Lind, *Methods of Structural Safety*, Prentice-Hall Inc., Englewood Cliffs, New Jersey, 1986.
- [14] Hohenbichler, M. and R. Rackwitz, 'Nonnormal Dependent Vectors in Structural Reliability,' *Journal of the Engineering Mechanics Division*, ASCE, Vol. 107, 1981, pp. 1227-1238.
- [15] Hohenbichler, M., 'An Asymptotic Formula for the Probability of Intersections,' *Berichte zur Zuverlässigkeitstheorie der Bauwerke*, Heft 69, LKI, Technische Universität München, 1984, pp. 21-48.
- [16] Breitung, K., 'Asymptotic Approximations for Multinormal Integrals,' *Journal of the Engineering Mechanics Division*, ASCE, Vol. 110, 1984, pp. 377-386.
- [17] Hohenbichler, M., Gollwitzer, S., Kruse, W., and R. Rackwitz, 'New Light on First- and Second-Order Reliability Methods,' Manuscript, Technical University of Munich, 1986.

- [18] Hohenbichler, M., 'Mathematische Grundlagen der Zuverlässigkeitsmethode Erste Ordnung und Einige Erweiterungen,' Doctoral Thesis at the Technical University of Munich, Munich, West Germany, 1984.
- [19] Madsen, H. O., 'Random Fatigue Crack Growth and Inspection,' in *Structural Safety and Reliability*, Proceedings of ICOSSAR'85, Kobe, Japan, IASSAR, 1985, Vol. 1, pp. 475-484.
- [20] Madsen, H. O., 'Model Updating in First-Order Reliability Theory with Application to Fatigue Crack Growth,' in *Proceedings, Second International Workshop on Stochastic Methods in Structural Mechanics*, University of Pavia, Pavia, Italy, 1985.
- [21] Madsen, H.O., Skjong, R. and M. Moghtaderi-Zadeh, 'Experience on Probabilistic Fatigue Analysis of Offshore Structures,' in *Proceedings, OMAE Conference*, Tokyo, Japan, 1986, Vol.II, pp.1-8.

